ΣΥΝΕΔΡΙΑ ΤΗΣ 28ΗΣ ΝΟΕΜΒΡΙΟΥ 1996

ΠΡΟΕΔΡΙΑ ΙΩΑΝΝΟΥ ΠΕΣΜΑΖΟΓΛΟΥ

A plausible model for the explanation of the selectivity effect of seismic electric signals, *by P. Varotsos, N. Sarlis, M. Lazaridou, and P. Kapiris,* διὰ τοῦ 'Ακαδημαϊκοῦ κ. Καίσαρος 'Αλεξοπούλου.

ABSTRACT

Previous publications by other groups claim that, in order to detect Seismic Electric Signals (SES) at epicentral distances r≈100km, huge current intensities have to be emitted from the focal area. In this paper, we suggest a model, which explains that, even a current intensity of 1A, is sufficient to produce detectable SES at r≈100km. This model also indicates that SES can be detectable within certain areas *only*, thus explaining the selectivity effect. It is also shown that, for big earthquakes *only*, i.e., with M≈6.5-7.0, a magnetic field variation becomes detectable simultaneously with SES; this was the case of the SES that preceded the 6.6 Kozani-Grevena earthquake in Greece.

Also the physical basis of the ΔV/L-criterion is summarised in an Appendix; we emphasize that when the long dipoles are appropriately installed (i.e., in configurations suggested by VAN long ago), their measurements , when compared to those of the short dipoles, lead to an immediate recognition of noise (due to an artificial source lying up to several km far away).

In an additional Appendix, we also discuss *Gruszow et* al.'s [1996] claim that the SES correlated with the 6.6 Kozani-Grevena earthquake can be attributed to a nearby industrial source, which emitted a huge current; we show that their claim sharply contradicts the theory and the experimental facts. For example, if these SES were due to an industrial nearby source: (a) they should have been accompanied mainly by *horizontal* magnetic field variations, while the magnetic signal observed by *Gruszow et al.* [1996] was mainly on the *vertical* component and (b) the electric field variations should have reached an amplitude two orders of magnitude larger than that observed. Furthermore, *Gruszow et al.* [1996] misused the VAN data, e.g., by incorrectly applying the ΔV/L-criterion; thus none of their arguments appears to work.

INTRODUCTION

Various physical mechanisms have been proposed (e.g., *Lazarus* [1993], *Slifkin* [1993, 1996], *Teisseyre* [1995], *Morgan* [1990; 1996, private communication], *Varotsos and Alexopoulos* [1986]) for the generation of the Seismic Electric Signals (SES), that have been found to precede earthquakes (EQs) in Greece (for a recent review on SES see

Uyeda [1996], while *Park et al.* [1993] summarized the generation mechanisms). These signals have been detected up to distances of the order of 100km from the epicenter; plausible models for their transmission have been suggested by *Lazarus* [1996], and *Varotsos et al.* [1993]. However, some publications (e.g., *Bernard and Le Mouel* [1996]) claim that a transmission at such distances is questionable, as it requires unreasonably huge current intensities I in the focal area. It is one of the main scopes of the present paper to show that even small current intensities of I ~1A, can lead to detectable electric field values, but only at certain regions of the earth's surface (thus explaining the selectivity effect, reported long ago by VAN, e.g., see *Varotsos and Lazaridou*, [1991]).

A second scope of this paper is focused on the calculation of magnetic field (B) variations accompanying the SES. VAN group repeatedly published that SES are not accompanied by *observable* variations of the *horizontal* components of the magnetic field (e.g., *Varotsos et al.* [1996a,b]), thus leading to an easy discrimination of SES from the usual magnetotelluric (MT) variations. The above does not imply that SES are not accompanied at all by magnetic field variations (the existence of which is obligatory from Maxwell equations), but that they are very small [cf. drastically smaller than those, which produce MT electric field variations having comparable amplitude (and period) to the SES] and hence are not readily detectable. In other words, there is a question of detectability *only* of the magnetic field variations for the usual cases of M 5.0-5.5 at r~100km, or so; on the other hand, it is naturally expected that appreciably strong SES activities could be accompanied by *detectable* magnetic field variations. In the present paper, we show that a value of Bz~1nT, or so, is naturally expected for strong EQs with M 6.5-7.0; this was observed before the 6.6 Grevena-Kozani, but *Gruszow et al.* [1996] misused this observation as an evidence for an artificial origin of the relevant SES observed by VAN. In Appendix II we summarize additional reasons, which show that *Gruszow et al.*'s [1996] claim is not valid. Furthermore, in Appendix I we review the physical basis of the ΔV/L criterion suggested by VAN for discriminating true SES from signals of artificial origin; thus, the validity of this criterion for the SES associated with the aforementioned 6.6 earthquake excludes any possibility for these signals to be attributed to an artificial source.

THE MODEL FOR THE SES TRANSMISSION AT LONG DISTANCES

Varotsos and Alexopoulos [1986] and *Varotsos et al.* [1993] suggested the following model for the SES transmission: when the SES is emitted, the current follows the most conductive channel through which most of this current travels; if the emitting source lies near a channel of high conductivity (Fig. 1a) and our measuring station lies at a site (with appreciably higher resistivity than that of the conductive channel but) close to the top of the conductive channel, the electric field is appreciably stronger than in the case of a homogeneous, or horizontally layered earth; this indicates that signals may be detectable at larger epicentral distances, but not at shorter. Such a mechanism, as it will be shown below, explains the *selectivity* effect reported by VAN long ago, e.g., see *Varotsos and Lazaridou* [1991].

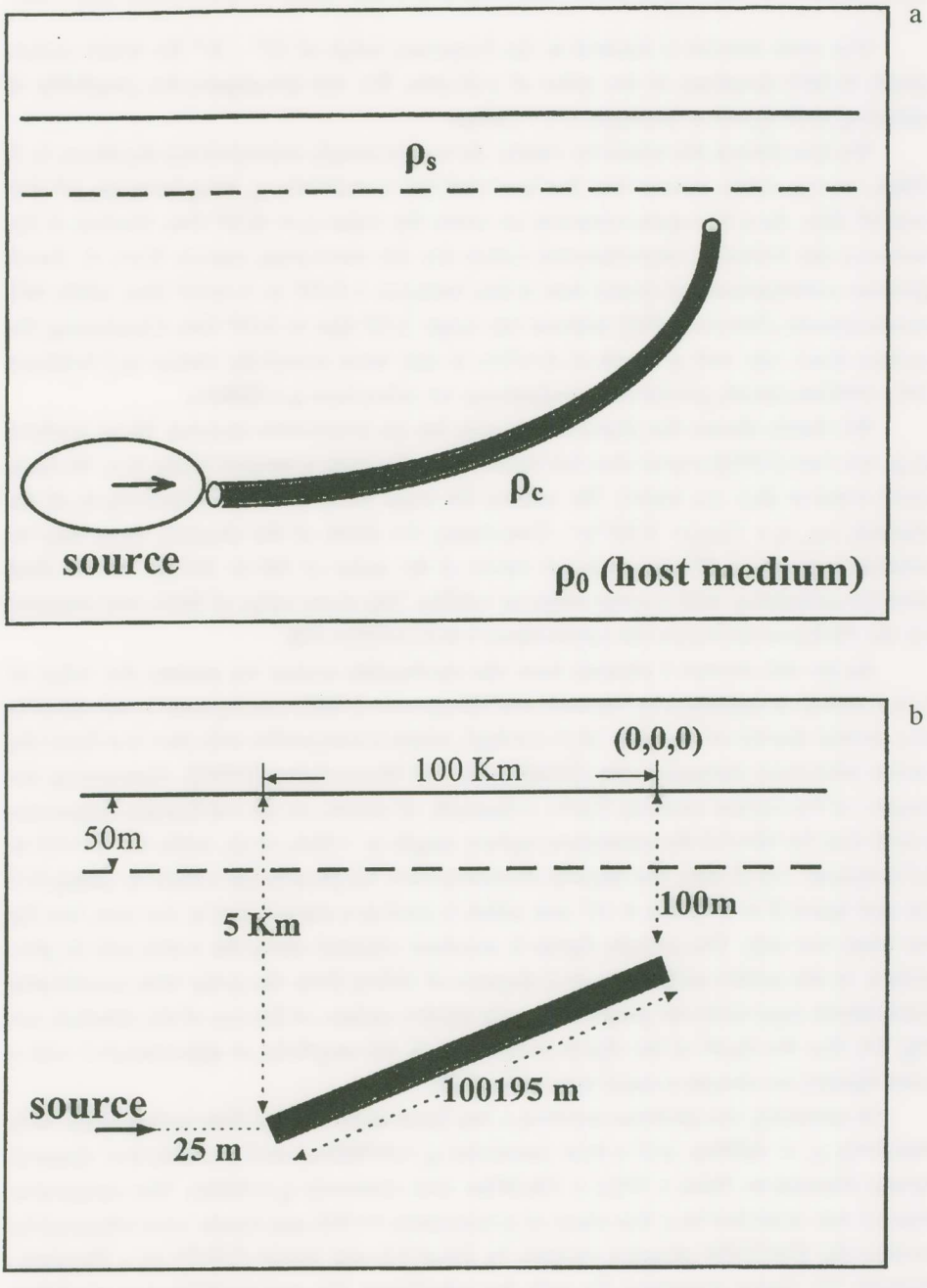

Fig. 1.a. The model (not to scale) of transmitting SES at long distances suggested by *Varotsos and Alexopoulos* [1986] and *Varotsos et al.* [1993]. Fig. b shows how the calculation is carried out: a thin sheet (of 500m×100km) with conductance 50S is considered.

SELECTION OF THE VALUES OF THE PARAMETERS USED IN THE CALCULATION

Our main interest is focused in the frequency range of 10^{-2} - 10^{-3} Hz which corresponds to SES durations of the order of 1-20 min. We will investigate the possibility of detecting such signals at distances of r ~ 100km.

We first discuss the resistivity values. As we are mainly interested for depths up to 5-30km, we can safely assume that the host rock has a resistivity ϱ_o lying between 10^3 Ωm and 10^4 Ωm. As a first approximation we select the value $\varrho_o \approx 4x10^3$ Ωm, because it lies between the following experimental values for the measuring station IOA: *K. Smith* (private communication) found that it lies between $1.5x10^3$ to $5.2x10^3$ Ωm, while MT measurements (Makris [1996]) indicate the range $3x10^3$ Ωm to $5x10^3$ Ωm. Concerning the surface layer, say with a depth of d≈50m, it may have resistivity values (ϱ_s) between 190 ~ 300Ωm (*Smith*, private communication); we select here $\varrho_s \approx 200\Omega$m.

We finally discuss the plausible values ϱ_c for the conductive channel. Many workers (e.g., see *Park* [1996]) report that the resistivity ϱ_f of a fault is around 10Ωm (i.e., 40 times more resistive than sea water). We assume the same value for the conductivity σ_c of the channel, i.e., $\sigma_c = (1/\varrho_f) = 0.1\Omega^{-1}m^{-1}$. Concerning the width of the channel, there may be contradictory views. We may assume values of the order of 100 to 1000m, but we shall start the calculation with a mean value of ≈500m. The same value of 500m was assumed for the thickness and hence the conductance τ is (0.1x500)=50S.

As for the current I emitted from the earthquake source we assume the value of I=1A which, as explained by *Varotsos and Alexopoulos* [1986], corresponds to an emission of a current density of the order of $j = 1A/km^2$, which is compatible with (but less than) the recent laboratory measurements (Hadjicontis and Mavromatou [1996]). Concerning the length *l* of the current emitting dipole, it depends, of course, on the earthquake magnitude (recall that for M≈5.0 the subsurface rupture length is ~5km, or so, while for M≈5.5 to 6.5 is around 7 to 25 km). For reasons of convenience, we present the results by taking *l*=1 km and hence *Il* ≈ 1Ax1km ≈ 10^3 Am which is used as a natural unit in our case, but for the main text *only*. The current dipole is assumed oriented along the x-axis and its projection on the earth's surface lies at a distance of 100km from the point with coordinates 0,0,0 (which represents the projection at the earth's surface of the top of the channel, see Fig. 1b). For the depth of the dipole source (which, for simplicity, is approximated with a point dipole), we assume a usual value of h=5km.

In summary, our problem involves a two layer earth (with a 50m surface layer with resistivity ϱ_s = 200Ωm, and a host resistivity ϱ_o=4000Ωm) and a conductive channel having dimensions 500m x 500m x 100,000m with resistivity ϱ_c=10Ωm. The conductive channel was modelled by a thin sheet of conductance τ=50S and results were obtained by running the EM1DSH program (written by *Hoversten and Becker* [1995]) on a Hewllett-Packard 735 digital computer. To help the calculation, the real problem was modelled according to the "similitude relationship" (*Zhdanov and Keller* [1994]), that relates the frequency ω, the magnetic permeability μ, the conductivity σ, and the length scale *l* of a

real world problem to a model problem,

$$\frac{\omega_m \mu_m \sigma_m \ell_m^2}{\omega_w \mu_w \sigma_w \ell_w^2} = 1 \qquad (1)$$

where the subscripts denote the real world (w) and the model (m) problem parameters.

In the following, we will calculate and discuss the variations of the amplitude of the electric and the magnetic fields appearing at various points x,y of the surface of the earth.

CALCULATION OF THE ELECTRIC FIELD VALUES

Figures 2 and 3 show plots of points of equal (absolute) values of the field strength. Fig. 2 depicts the contours of the horizontal component E_x of the electric field; for the schematic diagram depicted in Fig. 2a we used a grid of 5km x 5km, while for the detailed contours shown in Figs 2b and 2c more detailed grids, 2km x 2km and 2km x 0.5km respectively were considered. For example the contour labelled "1" shows the region at which E_x becomes $E_x \approx 1$ mV/km (cf. a symmetric region exists for negative values of y); Note that, in this example there is a large "shadow zone", i.e., $E_x < 1$ mV/km, lying between the two contours labelled "1". As a second example, we consider the case of selecting a threshold of E_x=10mV/km; again there are two regions, at which E_x is detectable, i.e., a region close to the top of the channel (with average dimensions 16km x 1km) and another one (roughly 8km x 10km) that includes sites lying at small distances from the source. Finally, if we consider appreciably larger values of E_x, e.g. $E_x \geq 28$mV/km, we find that E_x is detectable only at a narrow region close to the top of the channel. Figure 3 shows the contours for E_y; we see that the corresponding regions, at which E_y is detectable, have smaller dimensions when compared to those of E_x. Figs 4a and 4b show the variation of E_x and E_y at various distances (measured from the projection of the top of the channel on the earth's surface).

CALCULATION OF THE MAGNETIC FIELD VARIATIONS

A calculation, for $Il \approx 1$A x 1km (see Fig. 5), shows that the three components B_x, B_y, B_z **nowhere** exceed the detectable limit, which is usually around a few tenths of 1nT (cf., for a usual fluxgate variometer). Therefore, in order to achieve detectability of the magnetic field, a stronger source should be considered having two orders of magnitude larger value of Il; this corresponds to stronger EQs, e.g., with M≈6.5-7.0, or so. Note that, in such a case, the magnetic field becomes detectable at certain regions *only*, i.e., close to the epicenter (where $B_z \approx B_y > B_x$) or close to the top of the channel (where $B_z > B_y$). The first region might correspond to the observations of *Fraser-Smith* et al. [1990] (near the epicenter of the M_s 7.1 Loma Prieta EQ), while the second to the detection of ($B_z \approx 1$nT) at an epicentral distance of 70-80 km from the 6.6 Kozani EQ in Greece (*Varotsos et al.* [1996b,c]).

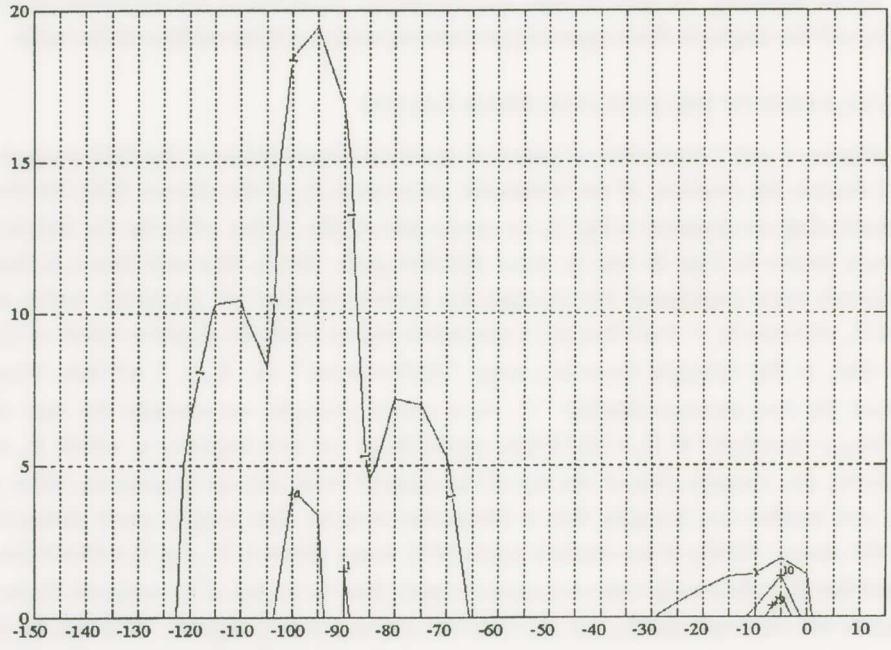

Fig. 2. Calculated values of the amplitude of the component E_x of the electric field: the contours correspond (from the outer to the inner): a) E_x: 1, 10, 19 mV/km; b) E_x: 1, 10, 19 mV/km; c) E_x: 1, 10, 19, 28, 37mV/km. Note that case (a) corresponds to a schematic diagram, while (b) and (c) to the detailed contours close to the epicenter and to the top of the channel respectively. (Note that the electric field values are calculated for a source 1km x 1A). The projection of the source on the earth's surface is x=-100km, y=0, while that of the top of the channel (see Fig 1b) corresponds to the origin (0,0).

b

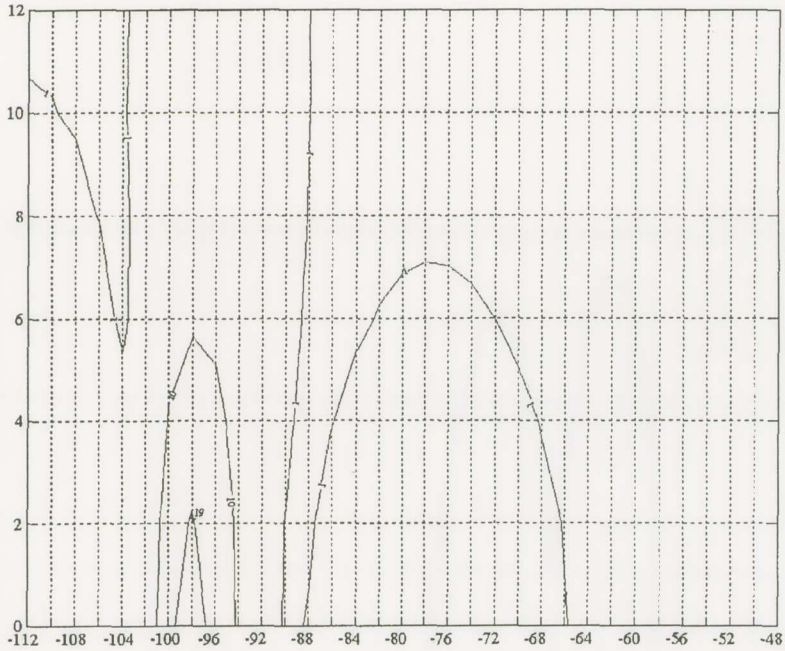
12
10
8
6
4
2
0
-112 -108 -104 -100 -96 -92 -88 -84 -80 -76 -72 -68 -64 -60 -56 -52 -48

c

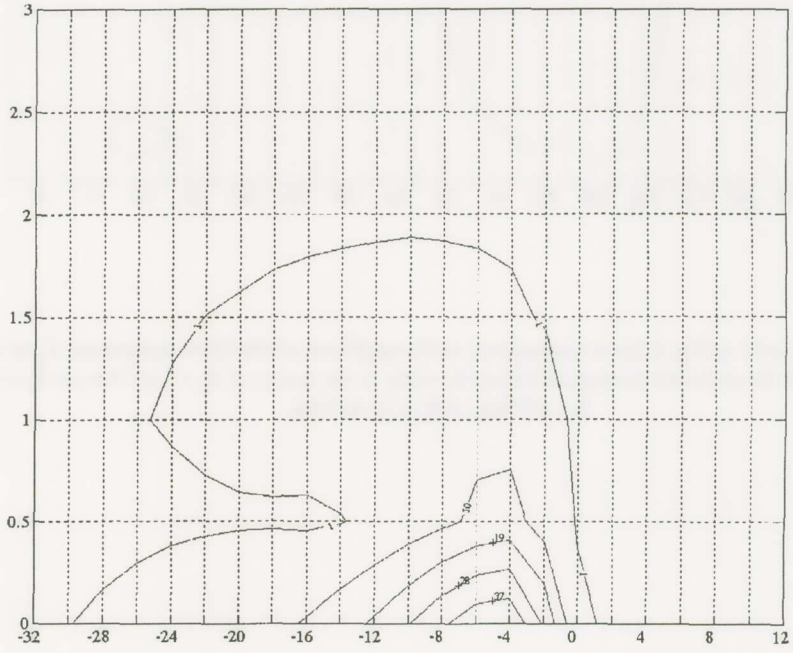
3
2.5
2
1.5
1
0.5
0
-32 -28 -24 -20 -16 -12 -8 -4 0 4 8 12

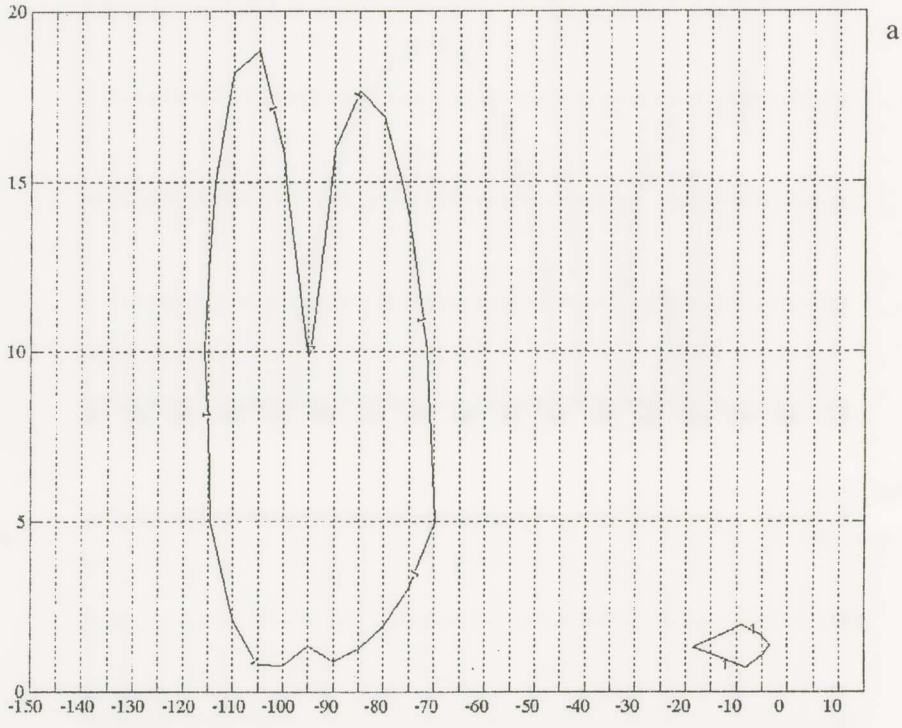

Fig. 3. The same as Fig. 2, but it corresponds to the amplitude of the other component E_y of the electric field; the contours correspond (from the outer to the inner): a) E_y=1 mV/km, b) E_y=1, 2, 3, ...mV/km, c) E_y=1,2 mV/km.

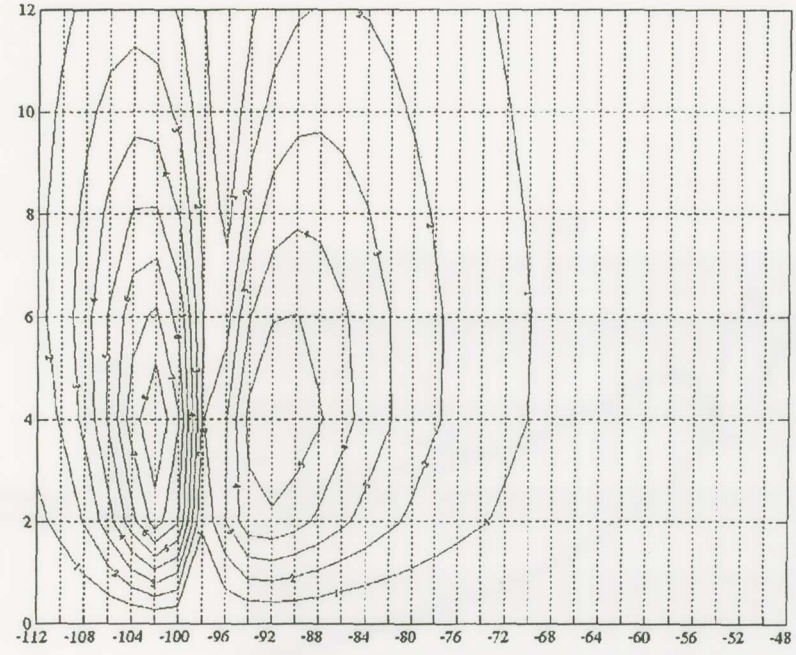
12
10
8
6
4
2
0
-112 -108 -104 -100 -96 -92 -88 -84 -80 -76 -72 -68 -64 -60 -56 -52 -48

b

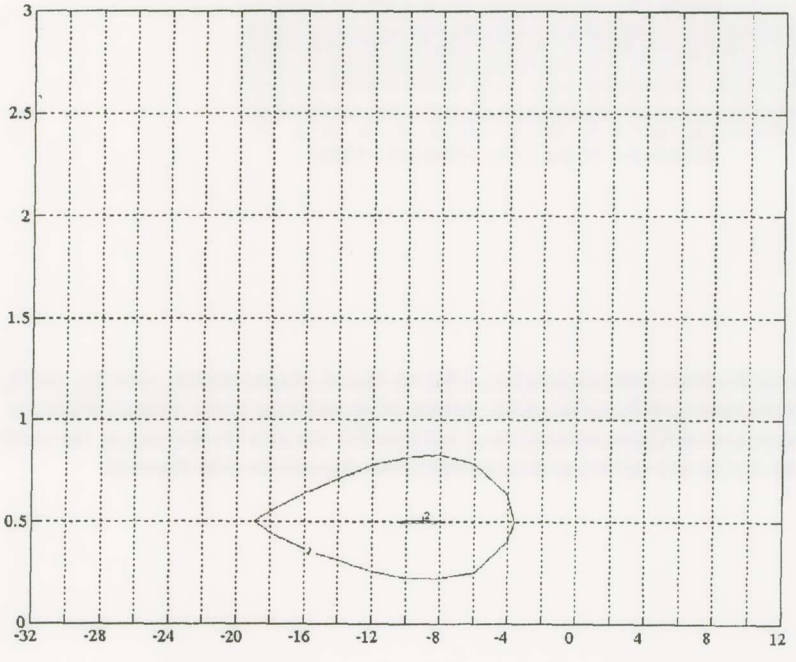
3
2.5
2
1.5
1
0.5
0
-32 -28 -24 -20 -16 -12 -8 -4 0 4 8 12

c

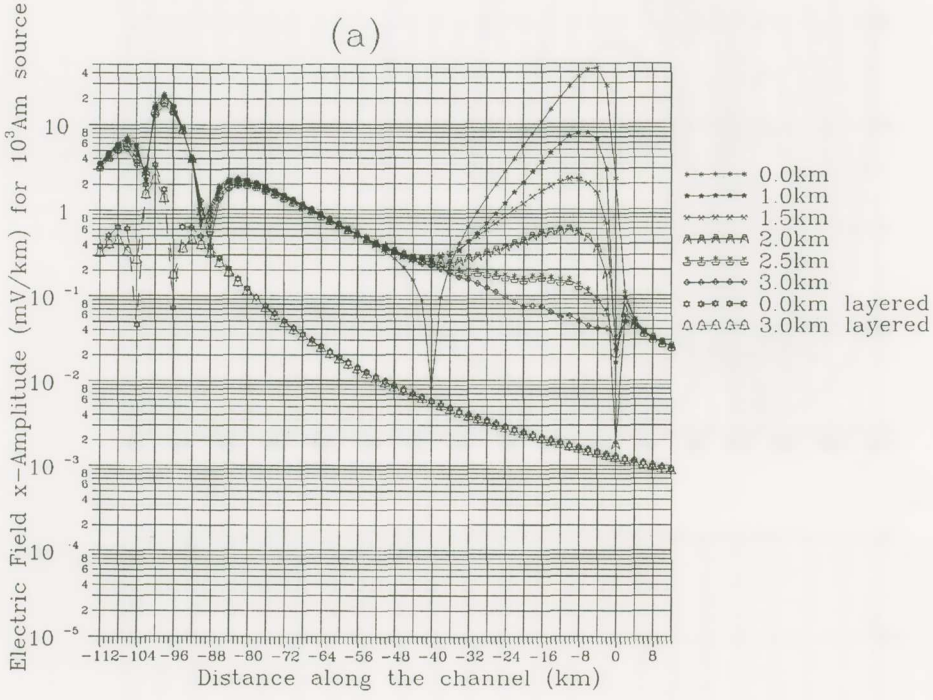

Fig. 4. Calculated values of the amplitudes, of the horizontal components E_x, case (a), and E_y, case (b), of the electric field on the earth's surface along and close to the channel. Different curves correspond to different values of the y-ordinate. For the sake of comparison, the results for the layered earth (and hence without the channel) are also depicted.

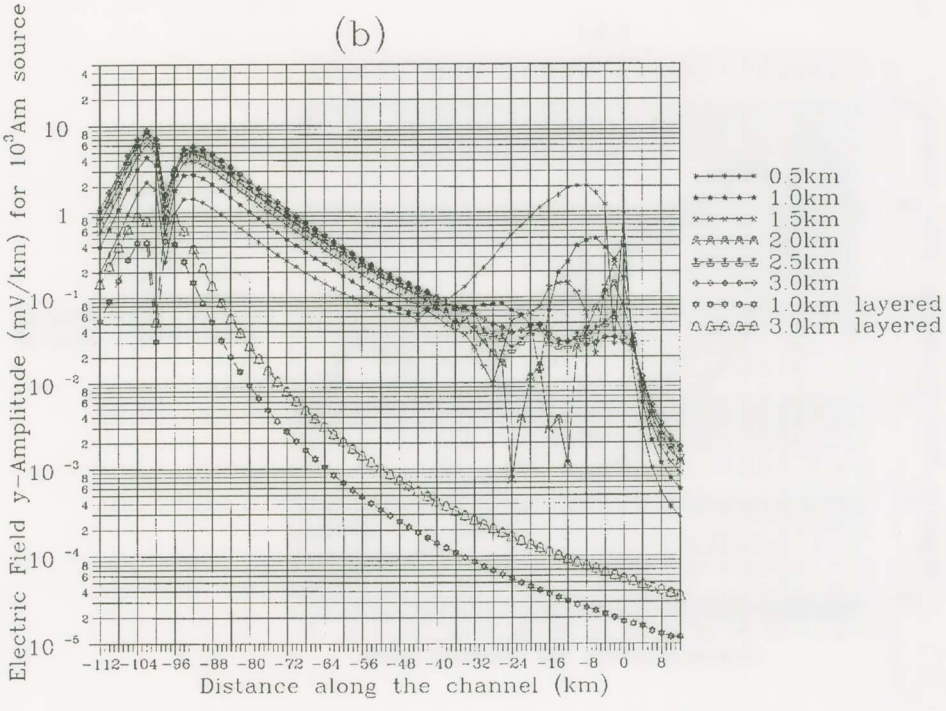
(b)
Electric Field y-Amplitude (mV/km) for 10^3Am source
Distance along the channel (km)
0.5km
1.0km
1.5km
2.0km
2.5km
3.0km
1.0km layered
3.0km layered

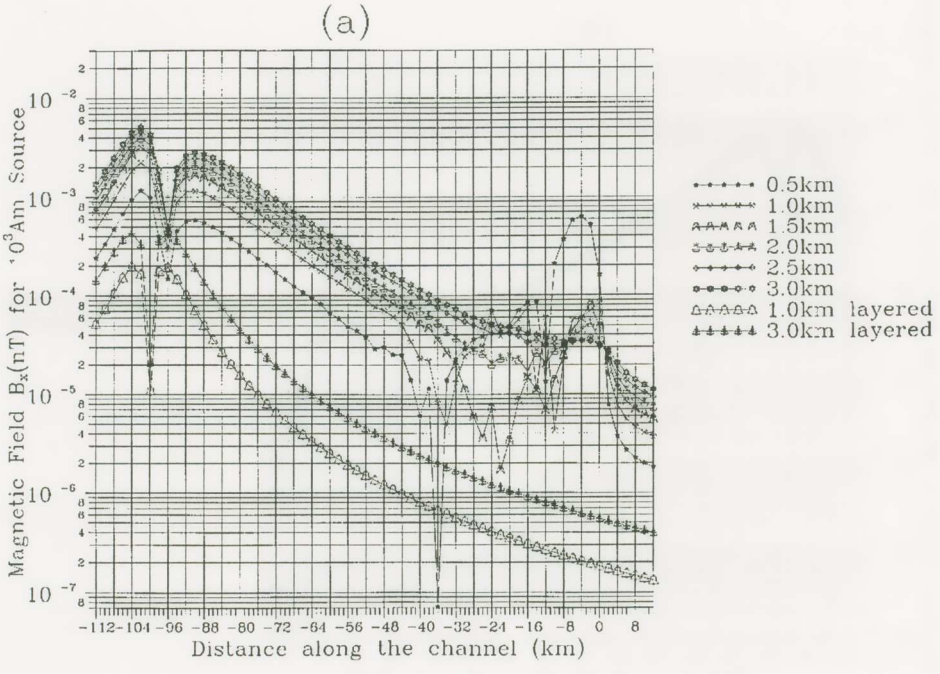

Fig. 5. Calculated values of the amplitudes of the three components B_x, case (a), B_y, case (b), B_z, case (c), on the earth's surface along and close to the channel. Different curves correspond to different values of the y-ordinate. For the sake of comparison, the results for the layered earth (and hence without the channel) are also depicted.

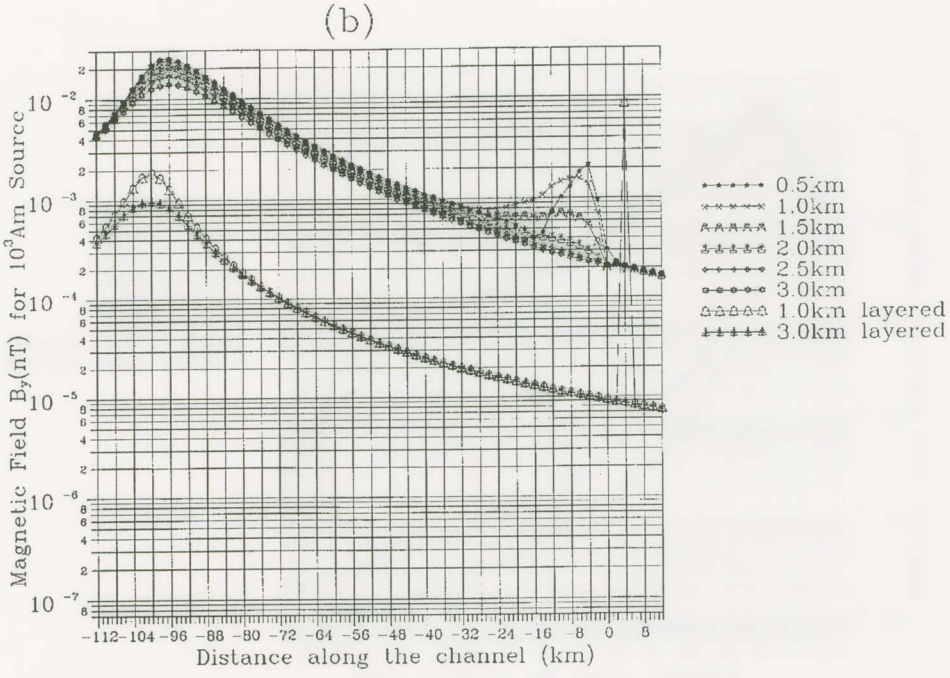
(b)
Magnetic Field B_y(nT) for 10^3Am Source
10^{-2}
10^{-3}
10^{-4}
10^{-5}
10^{-6}
10^{-7}
-112 -104 -96 -88 -80 -72 -64 -56 -48 -40 -32 -24 -16 -8 0 8
Distance along the channel (km)
0.5km
1.0km
1.5km
2.0km
2.5km
3.0km
1.0km layered
3.0km layered

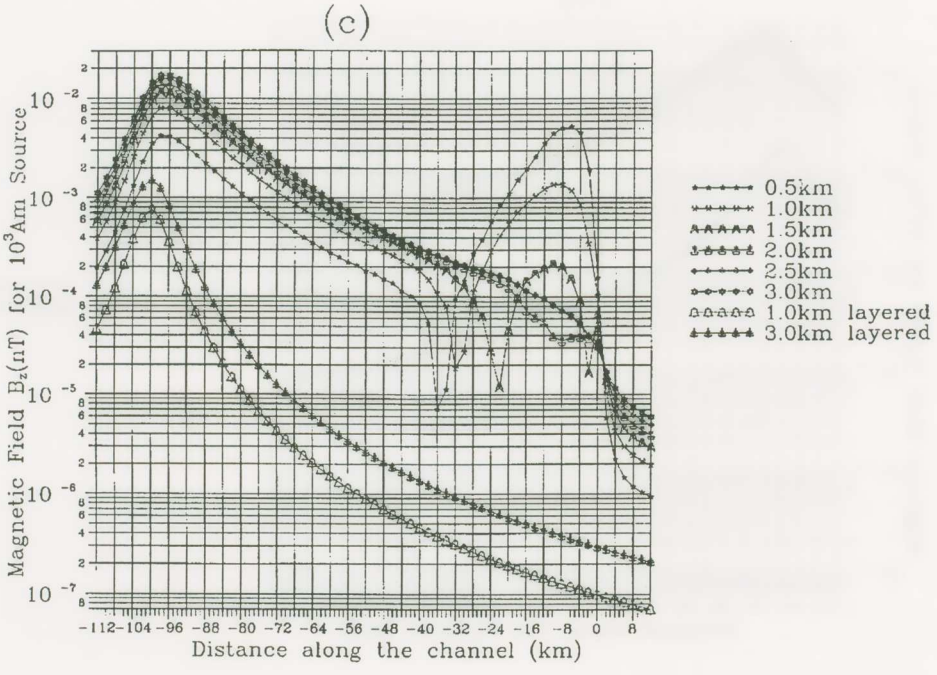
(c)
Magnetic Field B_z(nT) for 10^3Am Source
10^{-2}
10^{-3}
10^{-4}
10^{-5}
10^{-6}
10^{-7}
-112 -104 -96 -88 -80 -72 -64 -56 -48 -40 -32 -24 -16 -8 0 8
Distance along the channel (km)
0.5km
1.0km
1.5km
2.0km
2.5km
3.0km
1.0km layered
3.0km layered

DISCUSSION AND CONCLUSIONS

When considering that currents emitted in the earth should follow channels of reduced resistivity, we find a number of interesting results:

The first conclusion reveals that signals emitted from a current dipole 1A x 1km (at a depth of 5km) give detectable electric field values at distances of r≈100km, or so. Such electric signals are detectable on the earth's surface at certain regions *only*, which explains the *selectivity effect,* reported long ago by VAN (e.g., see *Varotsos and Lazaridou* [1991]).

A second conclusion emerging from the present calculation is that, for M≈5.0 - 5.5, the aforementioned electric signals can be observed without being accompanied by any observable variation of the magnetic field. On the other hand, when considering appreciably stronger EQs (e.g., M ~ 6.5-7.0), the magnetic field variations become observable (>0.25nT) at certain regions only, i.e., at short epicentral distances or close to the top of the conductive channel (e.g., at distances r ~ 100km); in the latter case, the vertical component B_z is appreciably larger than the horizontal component B_H. This feature is important, because it is quite different than what is (theoretically expected -see also Appendix II- and experimentally) observed when an artificial source emits current into the earth from distances of the order of a few km from the observation point; in other words, if magnetic field measurements show that B_z is significantly larger than B_H, this shows that the emitted signal cannot be due to a nearby artificial source. Concerning the latter point, note that once the long (measuring electric) dipoles, if they are properly installed (*Varotsos and Lazaridou* [1991]; *Varotsos et al.* [1993]), show approximately equal ΔV/L-values (cf. compatible with those of the short dipoles), the emitted signal cannot be ascribed to any nearby artificial source; the physical basis of the ΔV/L-criterion is reviewed in the Appendix I.

We should emphasize that the present results were derived on the basis of a thin sheet modelling; we think it necessary to repeat the calculation by using (other) 3D resistivity and EM modelling codes (cf. we are currently working in this direction).

The following remark should be added: the calculated values close to (0,0,0) could be questioned as they correspond to sites very near the conductive sheet (cf. we could overcome this, e.g., either by assuming that the thickness of the channel becomes less as we approach the measuring site*, or by increasing the depth of the top of the channel). We clarify however, that the aim of the present calculation is just to explain the correct order of magnitude of the electric field values, and also to show the general feature of the selectivity phenomenon.

The order of magnitude could be alternatively (i.e., without relying, as above, on any numerical solution of Maxwell equations) explained as follows. We first recall that laboratory experiments indicate that the current density emitted from the focal area (which have linear dimensions of, at least, a few km) is $\sim 10^{-5} A/m^2$ (or more). Second, field experiments show that the electric field values measured on the earth's surface, at r≈100km (for M ~ 6.0), are around 10mV/km, and hence the corresponding current density (at the

* The results remain the same if we decrease the thickness by a factor, e.g. 5, and simultaneously decrease the channel resistivity by the same factor (so that the conductance τ fo be constant, i. e., 50S).

measuring site) is around 10^{-7} to 10^{-8} A/m^2 (if we assume local resistivities of $10^2\Omega$m to $10^3\Omega$m respectively). In other words, what we must explain is a decrease of the current density, by 2-3 orders of magnitude, from the focal area to the measuring site; towards this scope, we may think as follows: Assume a conductive cylinder (ϱ_c), with radius R and infinite length, which is embedded in a more resistive medium (ϱ_0); if we consider an emitting current dipole (inside the cylinder and) along the cylinder axis (x), we can analytically calculate the electric field along that axis, at various distances r (see Appendix III). We then find that the value of E_x (inside the cylinder) decreases by three orders of magnitude (for a resistivity contrast $\varrho_c/\varrho_0 \sim 10/4000$) when increasing the distance from $r_1/R \approx 20$ to $r_2/R \approx 400$, or so (e.g., from $r_1 \approx$ 5km to $r_2 \approx$ 100km, if R=250m). As the electric field E_x inside (in) the cylinder, is equal to that just outside (out) it, i.e., $E_x^{in} = E_x^{out}$, it reflects that $j_x^{in}/ j_x^{out} \approx \varrho_0/\varrho_c \approx 4000/10$, at $r \approx r_2$, if the cylinder has an infinite length. If we assume, however, that the conductive cylinder terminates at $r=r_2$, we then expect a current density (to have an absolute value) of the order of $|j_x^{in}|$ at some points ($r \leq r_2$), within the host medium, lying close to the outcrop. Therefore, if the measuring site lies near the outcrop, the corresponding electric field $|E^{out}|$ should be of the order of $\varrho_0 x 10^{-3}$ xj($r=r_1$), which leads to measurable electric field values.

APPENDIX I. THE PHYSICAL BASIS OF THE ΔV/L-CRITERION. DISCRIMINATION OF TRUE SES FROM ARTIFICIAL SIGNALS WHEN USING A COMBINATION OF SHORT AND LONG DIPOLES.

VAN published four criteria according to which true SES can be discriminated from magnetotelluric (MT) variations and from anthropogenic disturbances (*Varotsos and Lazaridou* [1991]) (see *Nagao et al.* [1996] for a correct application of the four VAN criteria). The correct application of these criteria requires the simultaneous operation of short electric dipoles (e.g., with lengths L lying between 50 m and 200 m) and long dipoles (e.g., with L ≈ a few km to several km). As a general rule, we can state that **only** if the sites of the long dipoles are *properly* selected, with respect to the artificial sources (e.g., see Fig. 12 of *Varotsos and Lazaridou* [1991] or Appendix II and sections 3.2 and 3.3 of *Varotsos et al.* [1993]), can we achieve an easy discrimination of true SES from artificial signals emitted from distances up to several kilometers. Below we shall review the physical basis of the ΔV/L-criterion when long dipoles and short dipoles are simultaneously operating.

Consider a short (measuring) dipole AB (e.g., L=50m) and a long (measuring) dipole AΓ (e.g., L=5km) which lie on a straight line; although we assume here, for simplicity, that these dipoles have a common electrode A, this never occurs in practice, because we use independent neighbouring electrodes in order to avoid the simultaneous appearance of electrochemical noise, e.g., due to rain. We designate with ρ the distance of a (point) noise source from the *measuring* site (which, by definition, is the site of the short dipoles' deployment), while φ denotes the angle between the position vector of the noise and the direction of the measuring dipoles. If the noise source is an emitting current

(point) dipole (grounded on the earth's surface), θ denotes the angle between its dipole moment and the measuring dipoles (see Fig. AI.1). In the following we assume that the two measuring dipoles and the noise source lie on a straight line, i.e., $\varphi=0$ or $\varphi=180°$. These two cases are separately discussed.

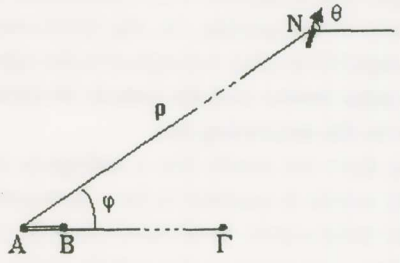

Fig. AI.1. Definition of angles φ and θ (and the distance ρ of the emitting dipole from the measuring site) when using a long dipole AΓ and a short dipole AB.

The calculations (static as we are in the near field approximation for $f\sim 10^{-3}$Hz) were performed by using the method of image charges. The series of image charges contributions was summed up numerically so as to obtain an accuracy of 1ppm. The results of the present calculation were compared to the results obtained by the Berkeley program (*Hoversten and Becker* [1995]) and showed a discrepancy of approximately 100ppm. This small discrepancy is due to the fact that the Berkeley program calculates the fields for $f=10^{-3}$Hz -and not for the steady-state- and to the integration algorithm that has to be used in order to calculate ΔV from the electric fields that are obtained from Berkeley's program.

As it is well known (*Zhdanov and Keller* [1994]), a source at the surface of a two layer Earth causes a series of image charges sited at an one-dimensional lattice with lattice constant 2d, where d is the depth of the surface layer, along the vertical line going through the source and with magnitudes diminishing according to the geometric progression K^n_{0S}, where n is the distance of the image charge from the source measured at lattice constants and $K_{0S}=(\varrho_0-\varrho_S)/(\varrho_0+\varrho_S)$. Thus, the electric potential for a monopole source of current I is

$$\varphi_m(\mathbf{x})=(\varrho_S I/2\pi)\ (1/|\mathbf{x}|)+\textit{Image sources contributions}$$

and for a point dipole current source **Π**, $|\mathbf{\Pi}|=Il$

$$\varphi_d(\mathbf{x})=(\varrho_S/2\pi)\ (\mathbf{\Pi}.\mathbf{x}/|\mathbf{x}|^3)+\textit{Image dipoles contributions}$$

The ΔV/L-value for the long measuring dipole AΓ, for example, is just $\{\varphi(A)-\varphi(\Gamma)\}/L$, where L is the length (AΓ). In *all* the calculations of this Appendix we shall assume I=1A and l=1m (instead of l=1km used in the main text). The calculation is made in each case: (i) either by representing the earth with a half-space, having resistivity $\varrho_0=4\text{x}10^3\Omega$m, or (ii) with a two (*horizontally*) layered earth having a surface layer (thickness ~50m) with

resistivity ϱ_s=200Ωm (and/or 10Ωm depending on the case) and a lower layer with ϱ_0=4x10^{3}Ωm.

The following three quantities are plotted in each figure: the ΔV/L-values recorded by the short dipole (L=50m) and the long dipole (L=5km), as well as their ratio, i.e., "ΔV/L of the long dipole" / "(ΔV/L of the short dipole)"; the latter quantity, for reasons of brevity, will be labelled "*Ratio (Long/Short)*" and is depicted with a continuous line (it corresponds to the left vertical scale). The former two quantities, i.e., the ΔV/L-values, are depicted with a dotted line and broken line respectively (they correspond to the right vertical scale).

Case A (φ=0°). The noise source and the remote electrode of the long dipole lie on the same side in respect to the measuring site.

Figs. AI.2a and AI.3a show the results (for a half-space and the two-layer model respectively) when the noise source is assumed to be a monopole, while Figs. AI.4a and AI.5a correspond to a dipole noise source. In all these cases the results show, as expected, that at large distances [when compared to the length (AΓ) of the long dipole, i.e., $\varrho >> (A\Gamma)$], the "ratio (Long/Short)" is around unity; as we move from $+\infty$ to the measuring site and approach the site of the remote electrode Γ, the "ratio (Long/Short)" increases at values significantly larger than unity (cf. this is one of the cases *recommended by Varotsos and Lazaridou* [1991] for an easy recognition of the noise, see their Fig. 12c); for example, at distances two times larger than the (long) dipole length, i.e., $\varrho \sim 2(A\Gamma)$, the "ratio (Long/Short)" reaches the value ~2 for a monopole and ~3 for a dipole noise source. Note that these values hold irrespective of whether we consider half-space or a two-layer model (in the latter case, if we consider that the upper layer resistivity is very low, i.e., $\varrho_s \approx 10\Omega m$, the ratio under discussion still remains large, i.e., ~2, when $\varrho \sim 2(A\Gamma)$, for a dipole emitting source; see Fig. AI.6a).

At shorter distances from the measuring site, i.e., $\varrho < (A\Gamma)$, Figs. AI.4a and AI.5a show that (for a dipole emitting source) the "ratio (Long/Short)" takes negative values, thus leading to an even easier recognition of the noise source; at these distances, but for a monopole noise source, the ratio is appreciably larger than unity, when it lies at small distances from the remote electrode Γ, and becomes negative when $\varrho < (A\Gamma)/2$. Thus, we see that, in any case (i.e., irrespective if the noise comes from a monopole or a dipole current emitting source N), *the "ratio (Long/Short)" is negative* provided that $\varrho < (A\Gamma)/2$, i.e., the remote electrode Γ is installed so that for the noise source to lie closer to the measuring site (than the remote electrode Γ); this is the case (II) *recommended* in Fig. 22 by *Varotsos et al.* [1993a] (or in Fig. 12a,b by *Varotsos and Lazaridou* [1991]) for an easy recognition of the noise.

The aforementioned figures AI.4a, AI.5a and AI.6a show the results when the dipole moment is parallel to the measuring (long and short) dipoles, i.e., θ=0. The study was extended (for the half-space with ϱ_0=4x10^{3}Ωm) to various values of θ, i.e., from 0 to 180° and the results are depicted in Figs. AI.7 and AI.8, for steps every 10° (except for θ ~ 90°); although the ΔV/L-values change from case to case, the "ratio (Long/Short)" retains exactly the same behaviour as in Fig. AI.4a (or AI.5a); for example, note that this ratio is around 3 when $\varrho \sim 2(A\Gamma)$, or around 2 when $\varrho \sim 3(A\Gamma)$ (cf. both ΔV/L-values, for the short and long dipole, are positive for θ<90° and negative for θ>90°).

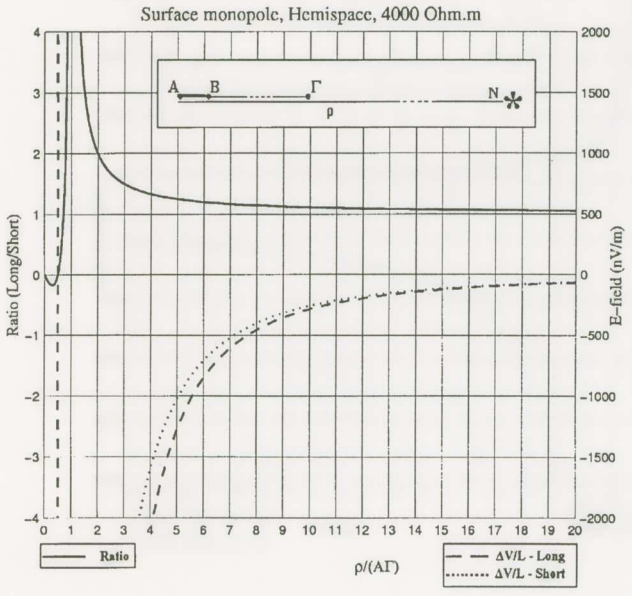

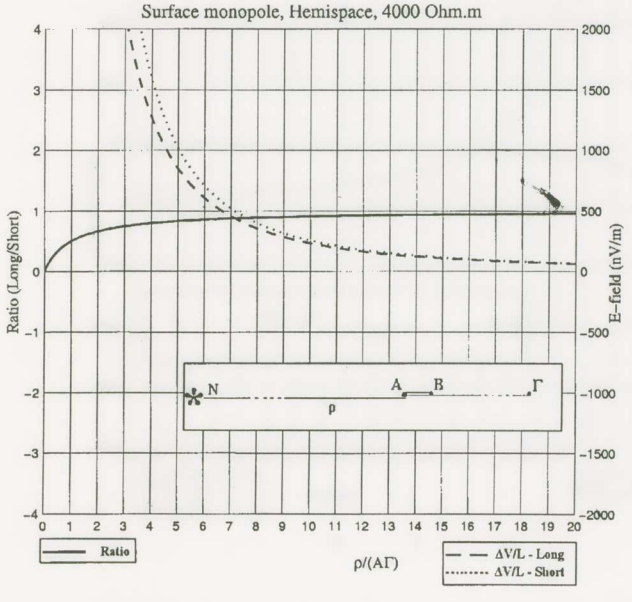

Fig. AI.2. The "ratio (Long/Short)" and the ΔV/L-values for a short dipole 50m and a long dipole 5km (cf. asymmetric dipoles) at various (reduced) distances from an emitting (surface) source. The calculation was made for a monopole source and a half-space ($\varrho_0=4x10^3\Omega m$); a: $\varphi=0$; b: $\varphi=180°$.

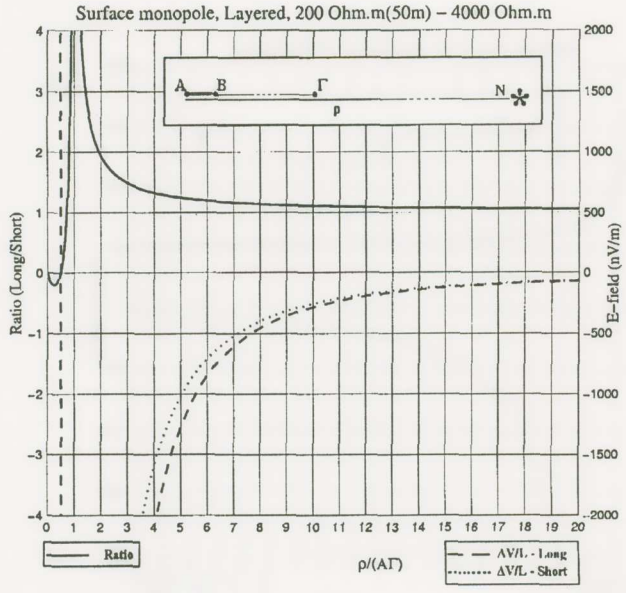

a

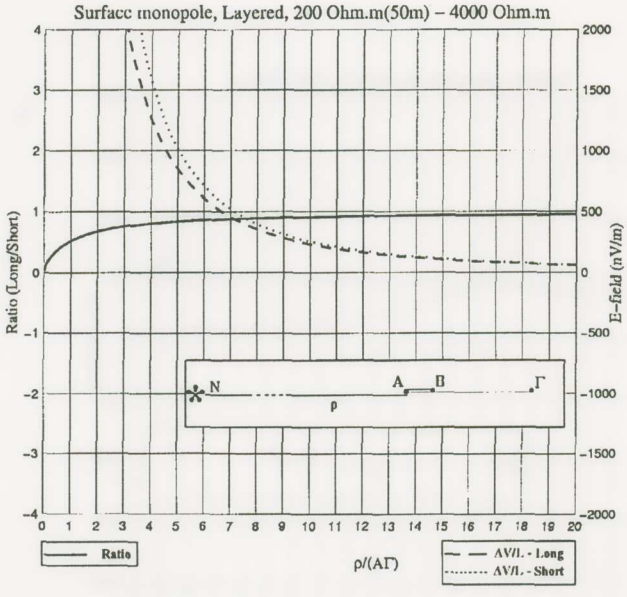

b

Fig. AI.3. The "ratio (Long/Short)" and the ΔV/L-values for a short dipole 50m and a long dipole 5km (cf. asymmetric dipoles) at various (reduced) distances from an emitting (surface) source. The calculation was made for a monopole source and a two layer earth (ϱ_S=200Ωm); a: φ=0; b: φ=180°.

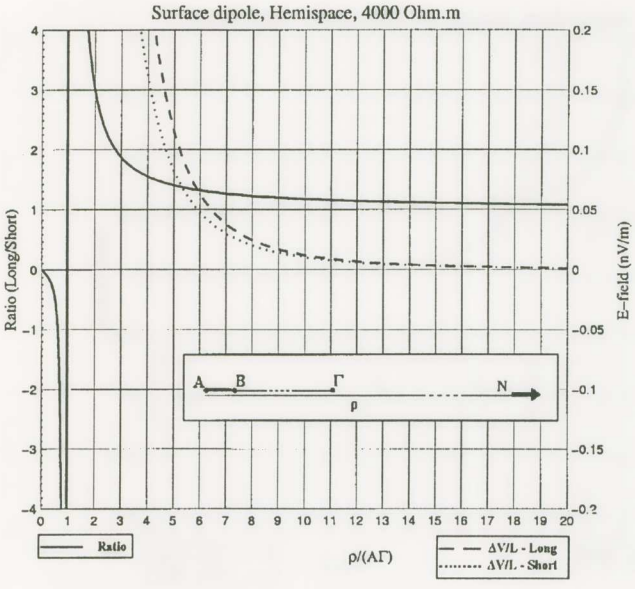

a

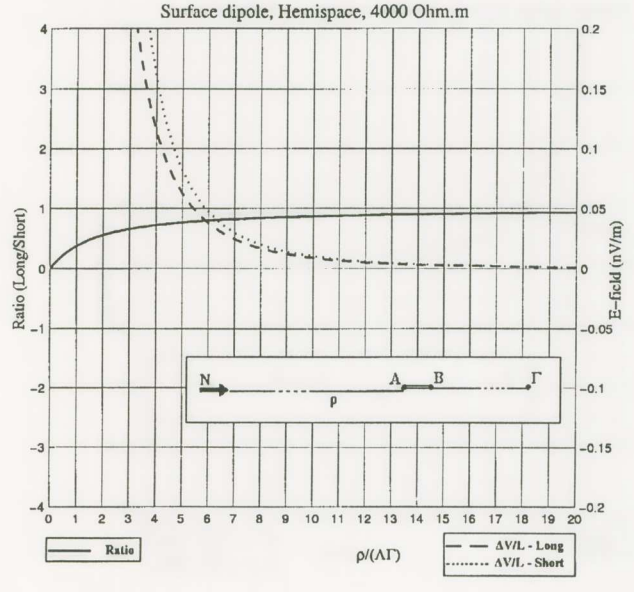

b

Fig. AI.4. The "ratio (Long/Short)" and the ΔV/L-values for a short dipole 50m and a long dipole 5km (cf. asymmetric dipoles) at various (reduced) distances from an emitting (surface) source. The calculation was made for a dipole source and a half-space ($\varrho_0=4x10^3\Omega m$); a: $\varphi=0$; b: $\varphi=180°$.

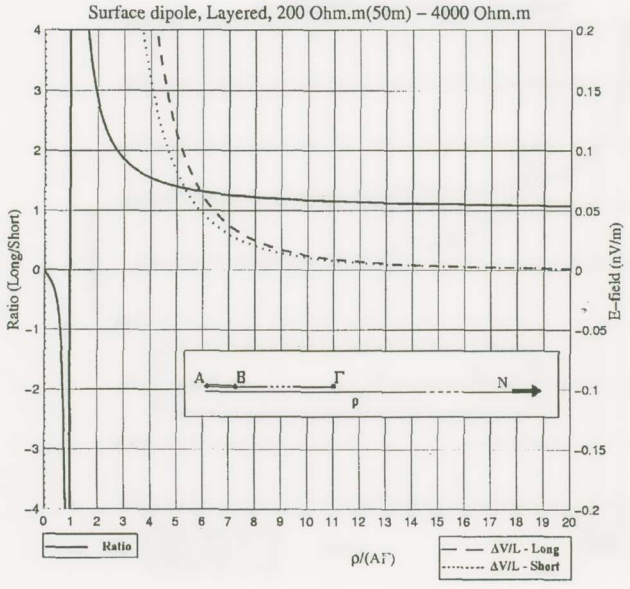

a

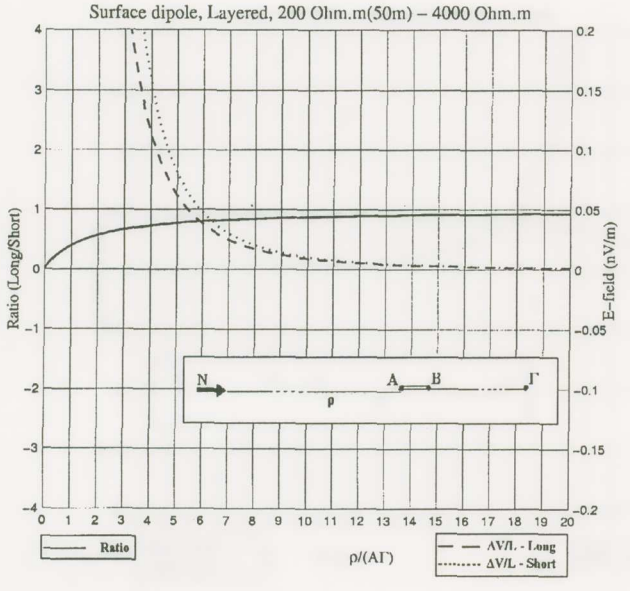

b

Fig. AI.5. The "ratio (Long/Short)" and the ΔV/L-values for a short dipole 50m and a long dipole 5km (cf. asymmetric dipoles) at various (reduced) distances from an emitting (surface) source. The calculation was made for a dipole source and a two layer-earth (ϱ_S=200Ωm); a: φ=0; b: φ=180°.

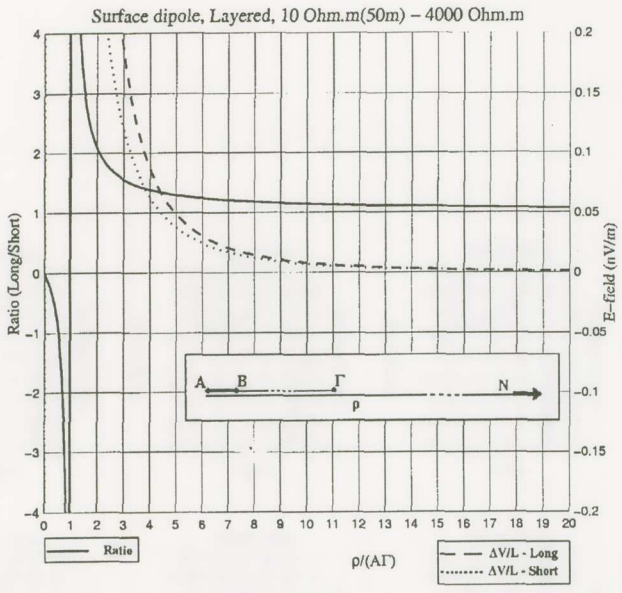

a

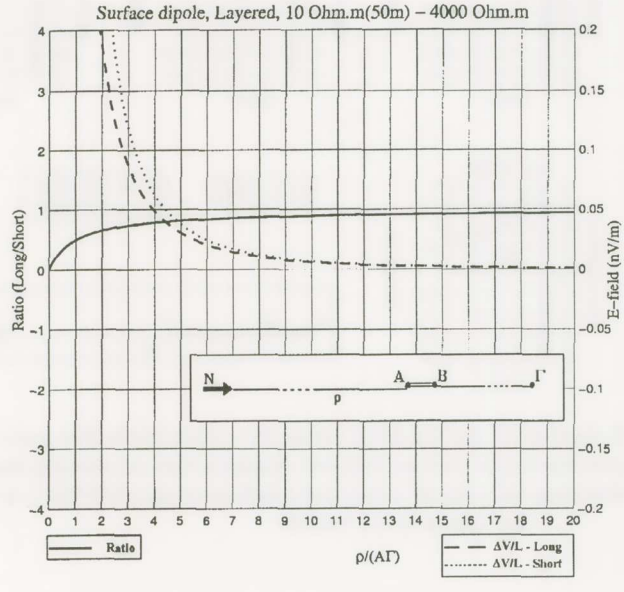

b

Fig. AI.6. The "ratio (Long/Short)" and the ΔV/L-values for a short dipole 50m and a long dipole 5km (cf. asymmetric dipoles) at various (reduced) distances from an emitting (surface) source. The calculation was made for a dipole source and a two layer-earth (ϱ_S=10Ωm); a: φ=0; b: φ=180°.

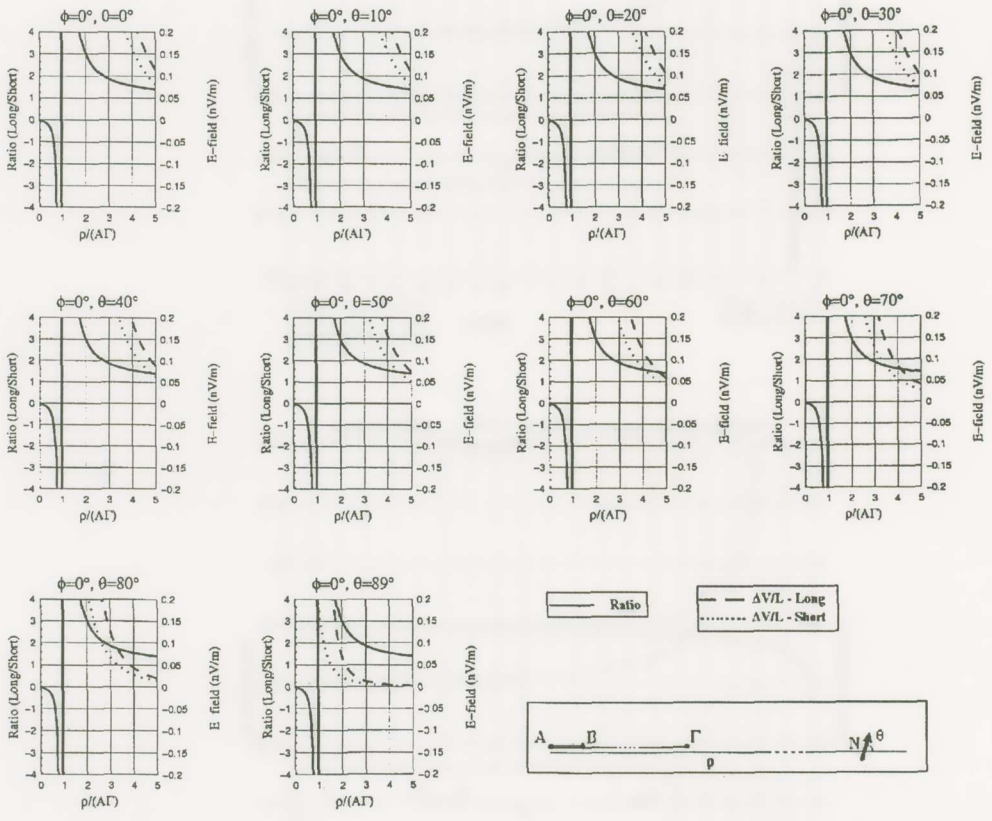

Fig. AI.7. The "ratio (Long/Short)" and the ΔV/L-values for a short dipole 50m and a long dipole 5km (cf. asymmetric dipoles) at various (reduced) distances from an emitting (surface) source. The calculation was made for a dipole source and a half-space ($\varrho_0=4x10^3\Omega m$); $\varphi=0$, but for various θ, i.e., θ=0-90°.

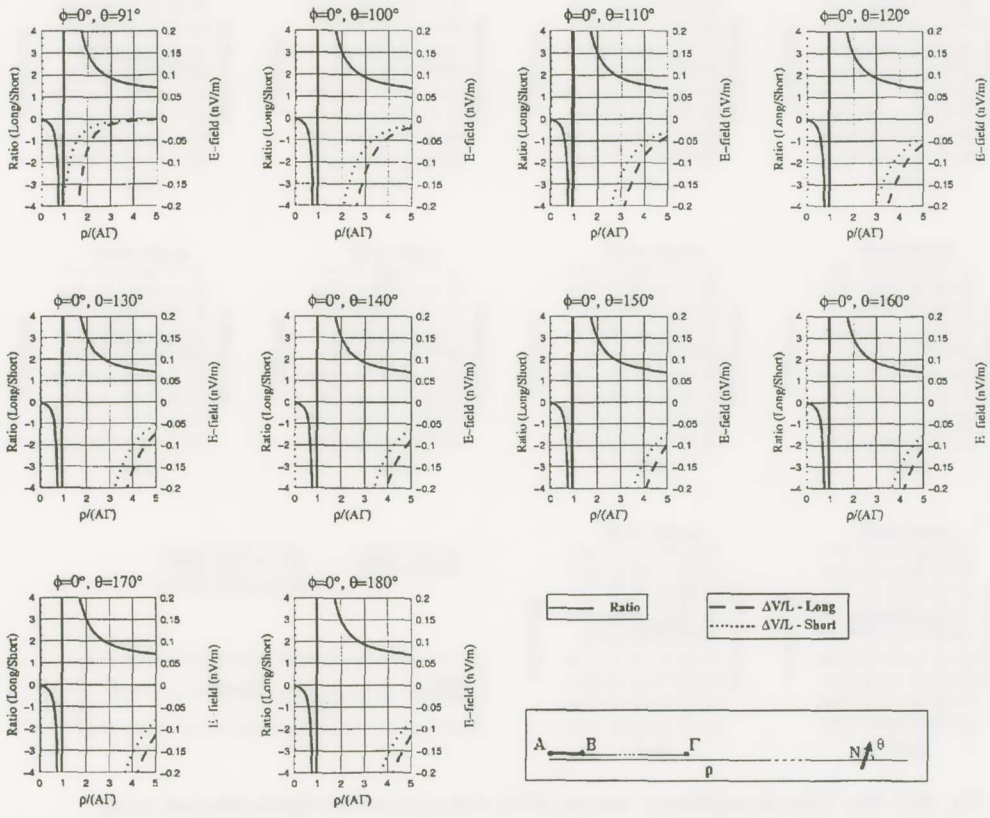

Fig. AI.8. The "ratio (Long/Short)" and the ΔV/L-values for a short dipole 50m and a long dipole 5km (cf. asymmetric dipoles) at various (reduced) distances from an emitting (surface) source. The calculation was made for a dipole source and a half-space ($\varrho_0=4x10^3\Omega m$); $\varphi=0$, but for various θ, i.e., θ=90°-180°.

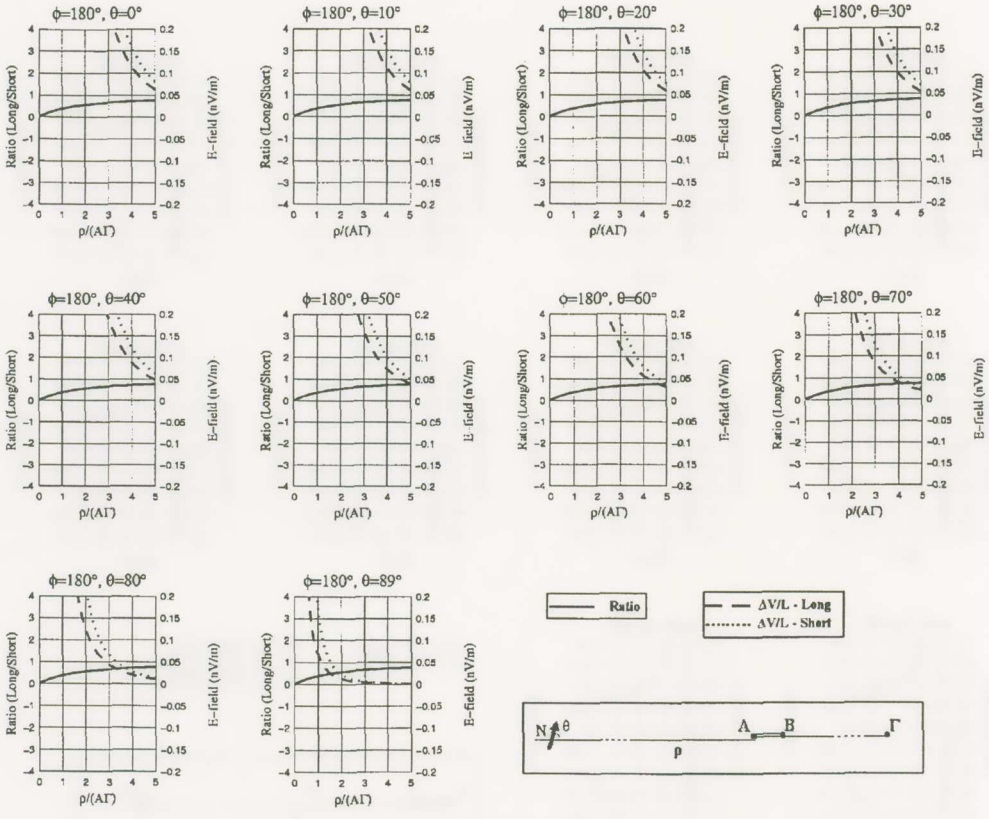

Fig. AI.9. The "ratio (Long/Short)" and the ΔV/L-values for a short dipole 50m and a long dipole 5km (cf. asymmetric dipoles) at various (reduced) distances from an emitting (surface) source. The calculation was made for a dipole source and a half-space ($\varrho_0=4x10^3\Omega m$); $\varphi=180°$, but for various θ, i.e., θ=0-90°.

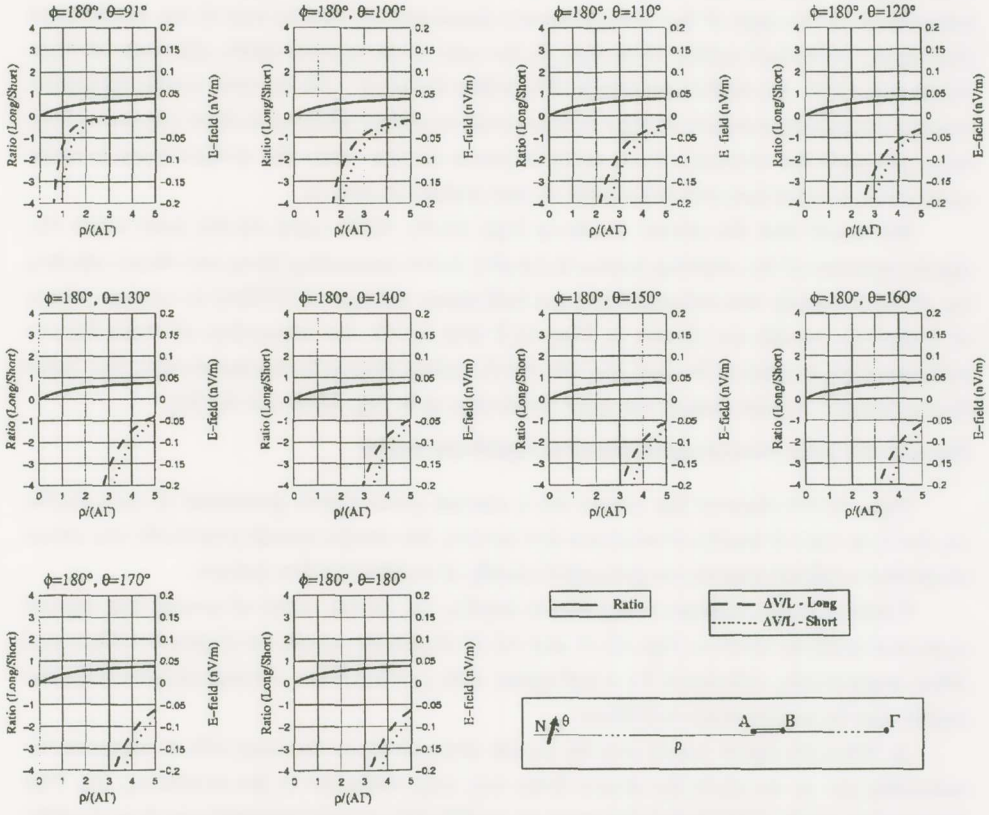

Fig. AI.10. The "ratio (Long/Short)" and the ΔV/L-values for a short dipole 50m and a long dipole 5km (cf. asymmetric dipoles) at various (reduced) distances from an emitting (surface) source. The calculation was made for a dipole source and a half-space ($\varrho_0=4\text{x}10^3\Omega\text{m}$); $\varphi=180°$, but for various θ, i.e., $\theta=90°\text{-}180°$.

Case B ($\varphi=180°$). The noise source lies at the other side, in respect to the measuring site, from the remote electrode of the long dipole

Figs. AI.2b and AI.3b refer to a monopole source, while Figs. AI.4b and AI.5b (and AI.6b) to a dipole source. In all cases the "ratio (Long/Short)" approaches unity, as expected, at large distances [i.e., $\varrho>>(A\Gamma)$]; although this ratio never becomes negative, it becomes markedly smaller than unity when the emitting source approaches the measuring site, e.g., $\varrho\sim 2(A\Gamma)$, and hence the noise becomes easily recognisable. This holds irrespective of the type of the current source (monopole or dipole) and of the model used (half-space or layered earth). Note that, in the case of the layered earth, although -in Figs. AI.5b and AI.6b- the surface resistivity differs by a factor of ~ 20, the ratio under discussion remains practically constant at large distances and is slightly affected at short distances only; more precisely the deviation from unity becomes smaller when the surface layer is more conductive, a behaviour which is similar to that noticed in case A.

We recall that the above results in Figs AI.4b, AI.5b (and AI.6b) hold when the dipole moment of the emitting source is parallel to the measuring (long and short) dipoles, i.e., $\theta=0$; the study was extended (for the half-space with $\varrho_0=4x10^3\Omega m$) to various values of θ and the results are shown in Figs AI.9 and AI.10. An inspection of these figures indicates that, in spite of the fact that the $\Delta V/L$-values change from case to case, the "ratio (Long/ Short)" retains exactly the same behaviour as in Fig. AI.4b (or AI.5b).

The case of a point current dipole buried at significant depths

Figs. AI.4-6 showed the results for a current point dipole grounded at zero depth, i.e., $h=0$; in case of depths of around a few meters, the results remain practically the same; recall that artificial sources are grounded usually at depths of a few meters.

Current dipole sources at significant depths, i.e., of the order of several km, cannot represent artificial sources; Figs AI.11 and AI.12 depict the results for depths $h=10$km and 30km respectively, calculated for a half-space with $\varrho_0=4x10^3\Omega m$. At such depths only, the results can be summarized as follows:

a) *When the dipole source and the remote electrode lie on the same side in respect to the measuring site:* as we move the source from very large distances to the measuring site, Figs AI.11a and AI.12a indicate that the "ratio (Long/Short)" remains continuously close to unity (but >1) only up to a point, the distance of which, from the remote electrode Γ becomes roughly equal with the dipole depth; at shorter distances, this ratio starts to decrease drastically and then follows the complicated behaviour depicted in Figs AI.11a and AI.12a.

b) *When the dipole source and the remote electrode lie on different sides in respect to the measuring site:* as we move from large distances to the measuring site, the ratio (Long/Short) remains continuously close to unity (but <1) only up to a point, having $\varrho\approx h$ (see Figs. AI.11b and AI.12b); at shorter distances, this ratio starts to drastically increase following the complicated behaviour depicted in Figs. AI.11b and AI.12b.

Note that for smaller depths, i.e., $h=5$km (which is comparable with the length of the measuring long dipole), the above behaviour is slightly different, as shown in

Figs AI.11c and AI.11d.

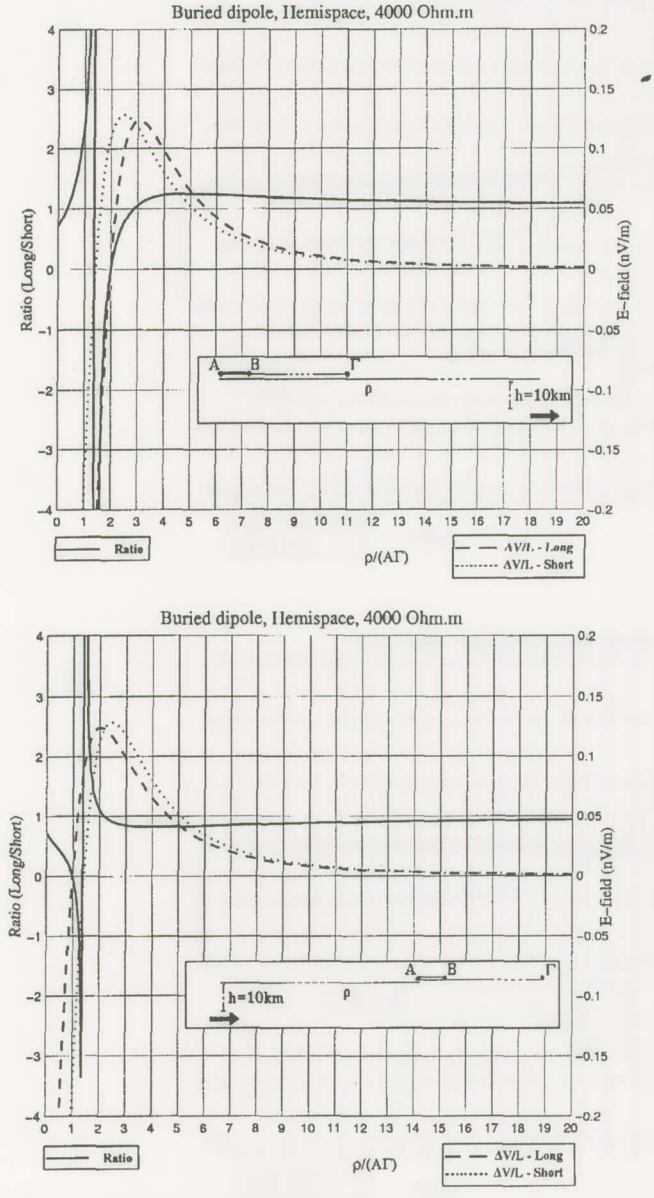

Fig. AI.11. The "ratio (Long/Short")" and the ΔV/L-values for a short dipole 50m and a long dipole 5km (cf. asymmetric dipoles) at various (reduced) distances from an emitting source. The calculation was made for a *buried* (h=10km) current dipole and a half-space ($\varrho_0=4x10^3\Omega m$); a: $\varphi=0$; b: $\varphi=180°$. For the sake of comparison, the calculation was repeated for a smaller depth h=5km (c: $\varphi=0$; d: $\varphi=180°$).

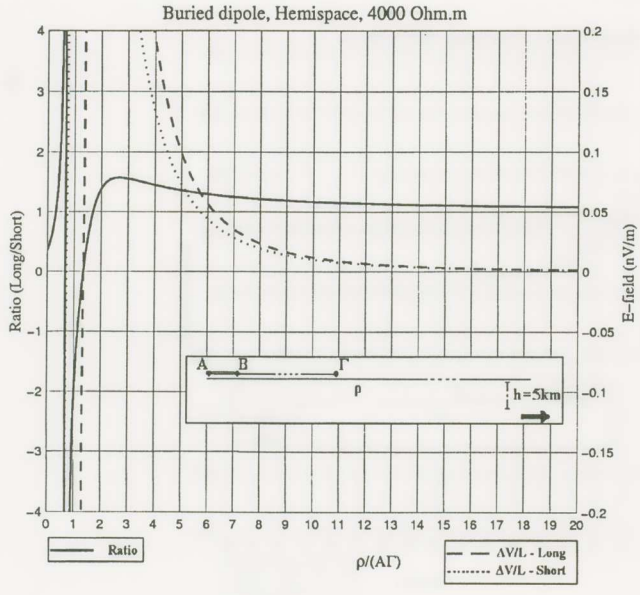
Buried dipole, Hemispace, 4000 Ohm.m
Ratio (Long/Short)
E-field (nV/m)
A
B
Γ
ρ
h=5km
Ratio
ρ/(AΓ)
ΔV/L - Long
ΔV/L - Short

c

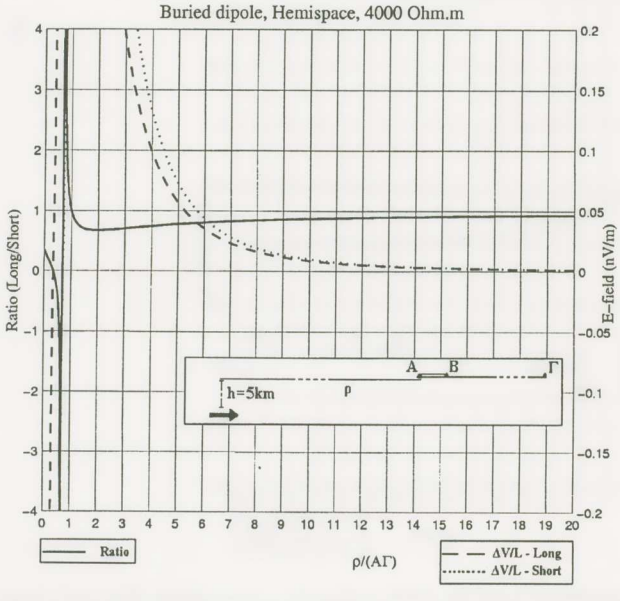
Buried dipole, Hemispace, 4000 Ohm.m
Ratio (Long/Short)
E-field (nV/m)
A
B
Γ
h=5km
ρ
Ratio
ρ/(AΓ)
ΔV/L - Long
ΔV/L - Short

d

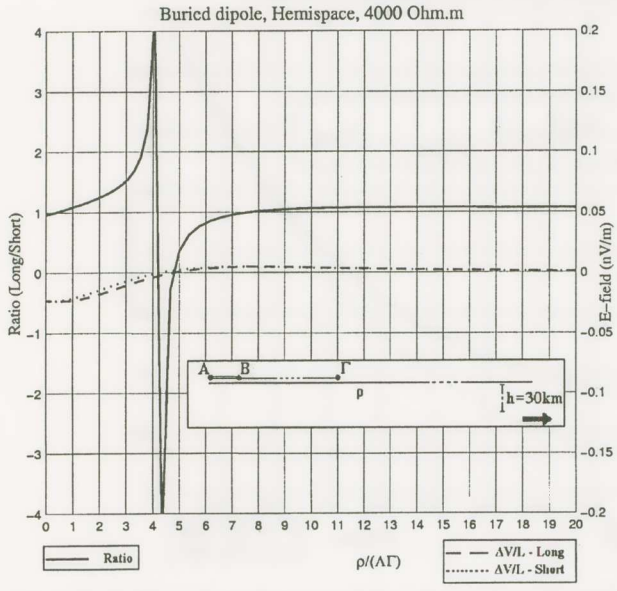

a

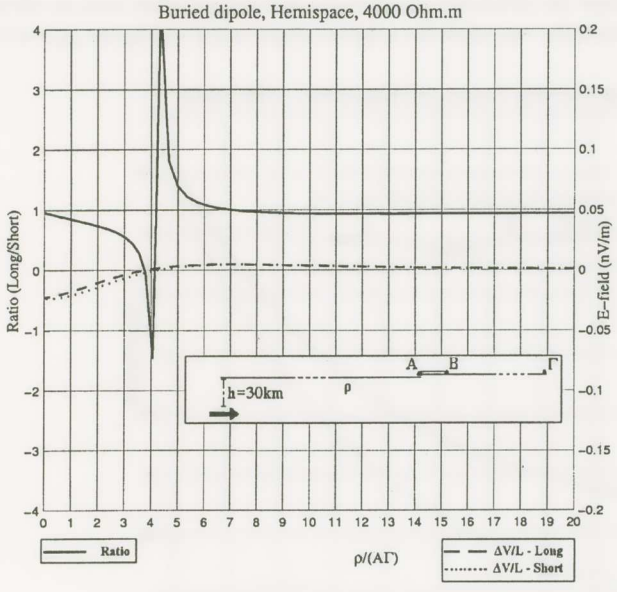

b

Fig. AI.12. The" ratio (Long/Short)" and the ΔV/L-values for a short dipole 50m and a long dipole 5km (cf. asymmetric dipoles) at various (reduced) distances from an emitting (surface) source. The calculation was made for a *buried* (h=30km) current dipole and a half-space ($\varrho_0=4x10^3\Omega m$); a: $\varphi=0$; b: $\varphi=180°$.

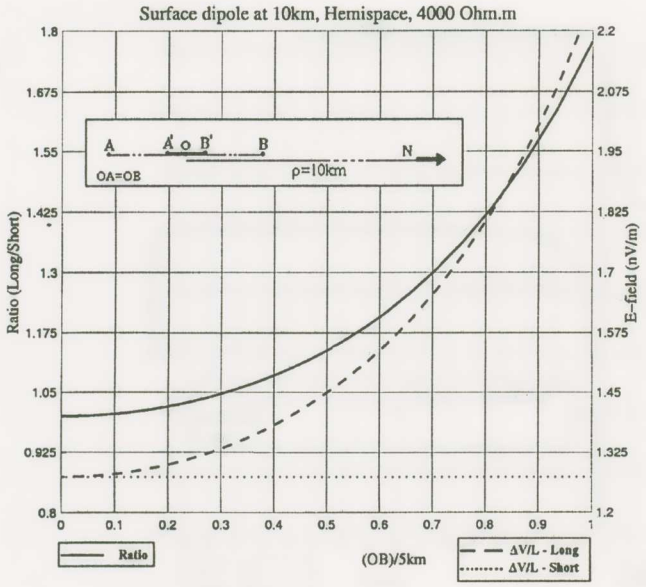

Fig. AI.13. The "ratio (Long/Short)" and the ΔV/L-values for a short dipole 50m and a long dipole *with variable length* (cf. symmetric dipoles) at a distance ρ=10km from an emitting (surface) source. The calculation was made for a dipole source and a half-space (ρ_0=4x10^{3}Ωm).

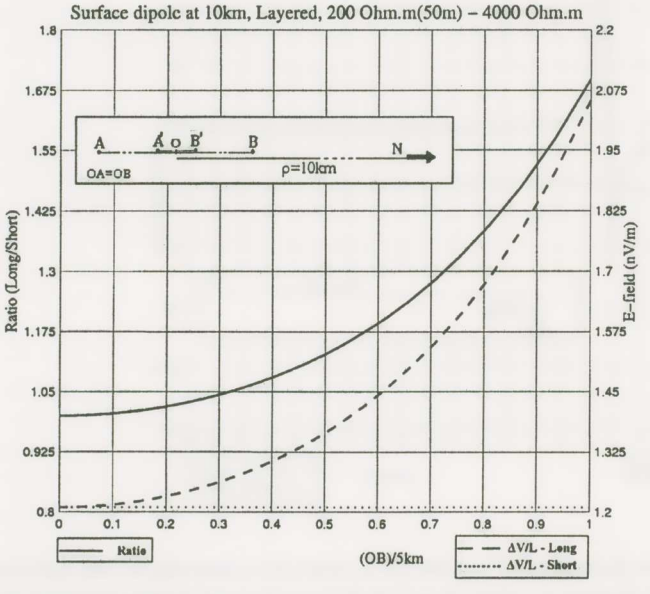

Fig. AI.14. The "ratio (Long/Short)" and the ΔV/L-values for a short dipole 50m and a long dipole *with variable length* (cf. symmetric dipoles) at a distance ρ=10km from an emitting (surface) source. The calculation was made for a dipole source and a two layer-earth (ρ_S=200Ωm).

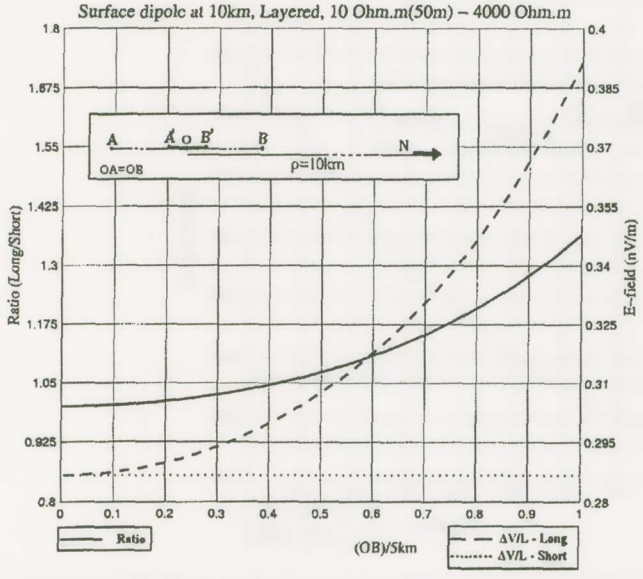

Fig. AI.15. The "ratio (Long/Short)" and the ΔV/L-values for a short dipole 50m and a long dipole *with variable length* (cf. symmetric dipoles) at a distance ρ=10km from an emitting (surface) source. The calculation was made for a dipole source and a two layer-earth (ϱ_S=10Ωm).

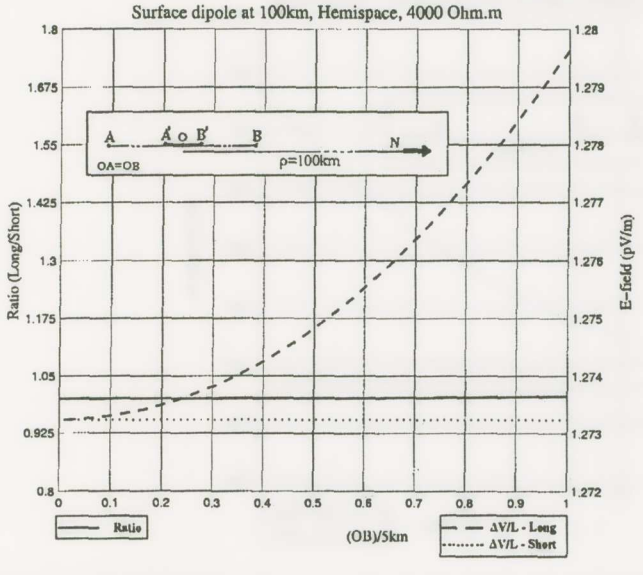

Fig. AI.16. The "ratio (Long/Short)" and the ΔV/L-values for a short dipole 50m and a long dipole *with variable length* (cf. symmetric dipoles) at a distance ρ=100km from an emitting (surface) source. The calculation was made for a dipole source and a half-space (ϱ_0=4x10³Ωm).

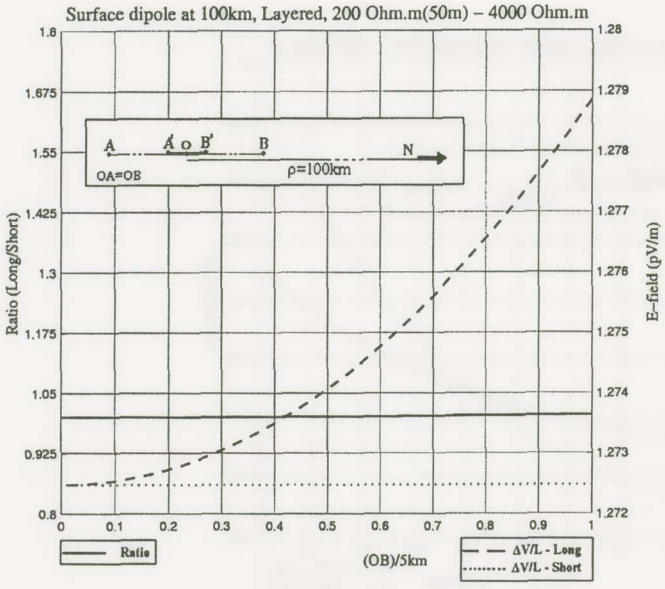

Fig. AI.17. The "ratio (Long/Short)" and the ΔV/L-values for a short dipole 50m and a long dipole *with variable length* (cf. symmetric dipoles) at a distance ρ=100km from an emitting (surface) source. The calculation was made for a dipole source and a two layer-earth (ϱ_S=200Ωm).

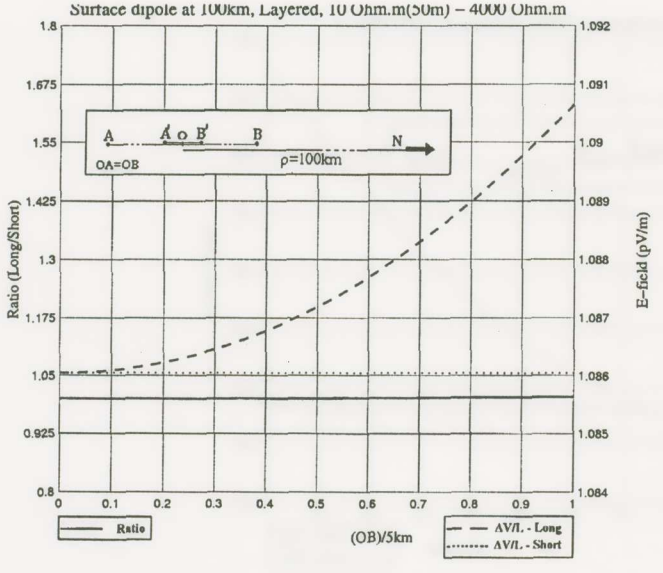

Fig. AI.18. The" ratio (Long/Short)" and the ΔV/L-values for a short dipole 50m and a long dipole *with variable length* (cf. symmetric dipoles) at a distance ρ=100km from an emitting (surface) source. The calculation was made for a dipole source and a two layer-earth (ϱ_S=10Ωm).

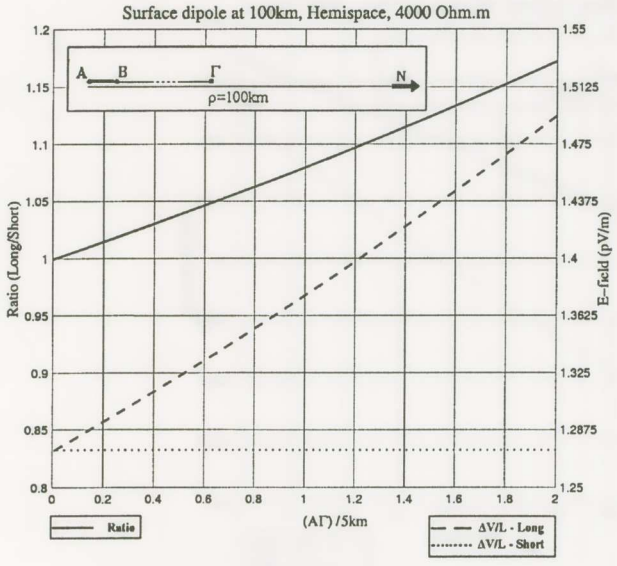

a

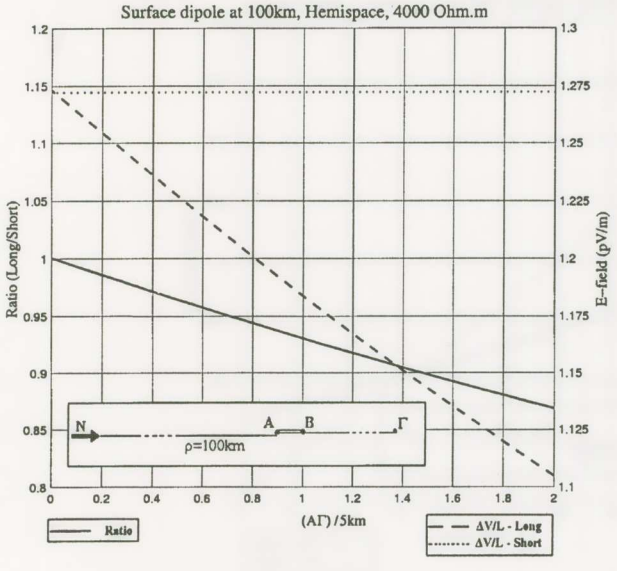

b

Fig. AI.19. The" ratio (Long/Short)" and the ΔV/L-values for a short dipole 50m and a long dipole *with variable length* (cf. asymmetric dipoles) at a distance ϱ=100km from an emitting (surface) source. The calculation was made for a dipole source and a half-space ($\varrho_0=4x10^3\Omega m$): a: φ=0; b: φ=180°.

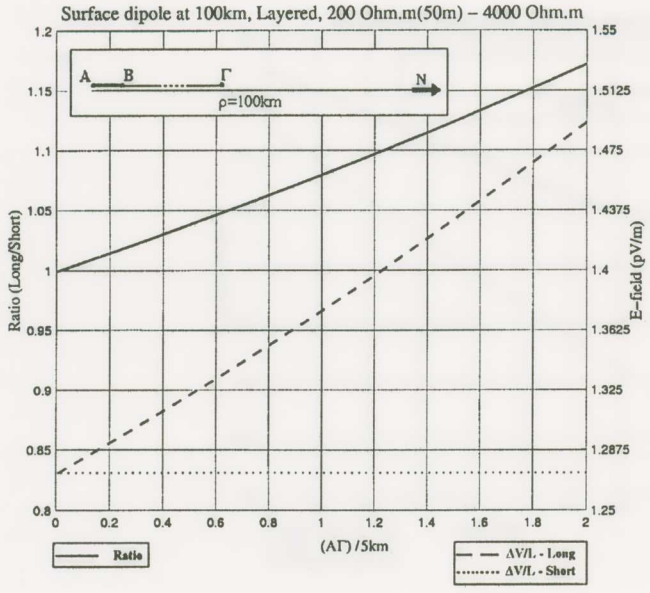

a

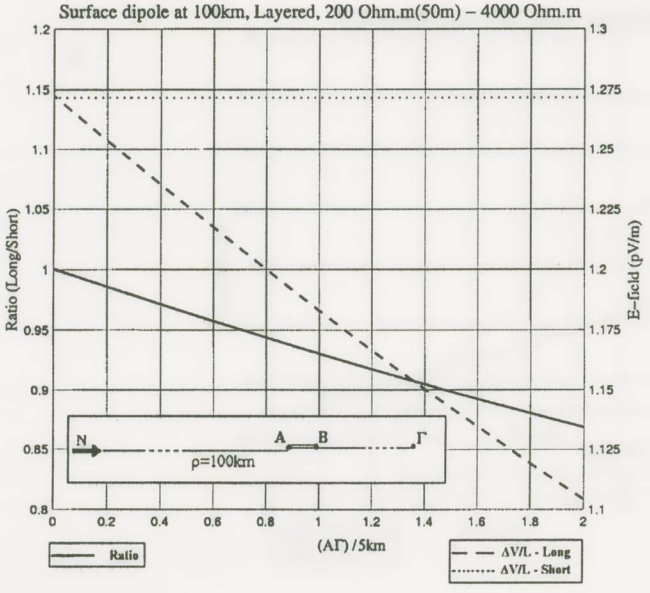

b

Fig. AI.20. The "ratio (Long/Short)" and the ΔV/L-values for a short dipole 50m and a long dipole *with variable length* (cf. asymmetric dipoles) at a distance ρ=100km from an emitting (surface) source. The calculation was made for a dipole source and a two layer-earth (ϱ_S=200Ωm): a: φ=0; b: φ=180°.

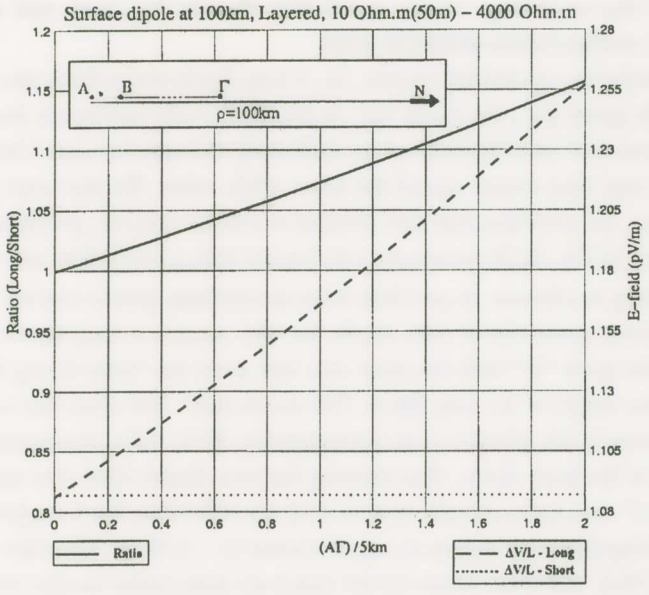

a

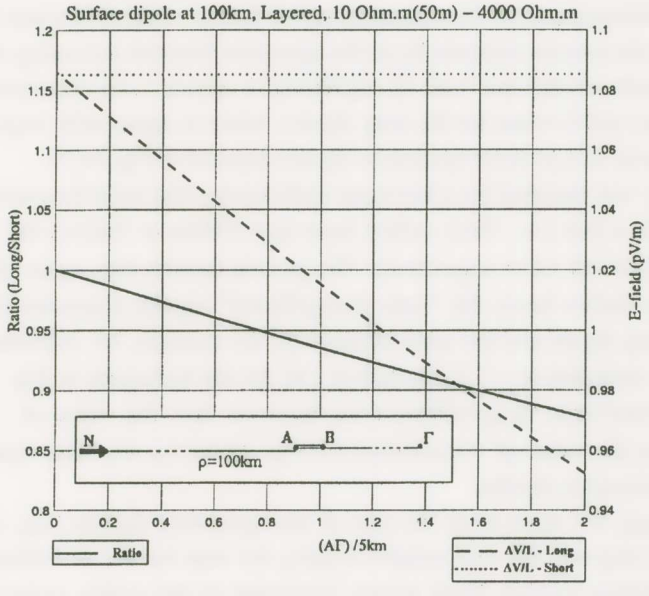

b

Fig. AI.21. The "ratio (Long/Short)" and the ΔV/L-values for a short dipole 50m and a long dipole *with variable length* (cf. asymmetric dipoles) at a distance ρ=100km from an emitting (surface) source. The calculation was made for a dipole source and a two layer-earth (ϱ_S=10Ωm): a: φ=0; b: φ=180°.

Comparison of the recordings of two symmetric dipoles (i.e., long and short). Why the asymmetric configuration should be used.

Let us now consider two symmetric dipoles, i.e., a long dipole and a short one, which have the same middle point (i.e., the point "O" in Figs AI.13-18) and lie on the same straight line; VAN never used such dipoles, but we shall study this case, because it has been erroneously reported that they always record the same ΔV/L-value. We first start with a relatively small distance, i.e., $\varrho \approx 10$km, and then proceed to a larger one, i.e., $\varrho \approx 100$km.

Case of $\varrho \approx 10$ km: In Fig. AI.13 we assume a half-space with $\varrho_0 = 4 \times 10^3 \Omega$m and a short dipole (A′B′)=50m lying at distance of $\varrho \approx 10$km from an emitting (point) current dipole (noise) source (Il=1Am), grounded at zero depth; we also assume a long dipole (AB), having the same middle point "O" with the short one, and study the "ratio (Long/Short)" for various values of the length of the long dipole. The results show that when this length is very small, in comparison to the distance ϱ, its corresponding ΔV/L-value almost coincides (as expected) to that of the short dipole, thus showing the true electric field. For example, the "ratio (Long/Short)" remains practically close to unity for AB≈1km, but for appreciably larger lengths (of the long dipole), it increases, e.g., it reaches to ~1.15 for AB≈5km and to ~1.42 for AB≈ 8km. Note that these values (of the ratio) are appreciably smaller when we compare them to the corresponding case of the asymmetric dipoles (cf. with the same lengths and the same distance ϱ from the measuring site) if they are located in a way so that the dipole source and the remote electrode lie on the same side from the measuring site; for example, Fig. AI.4a indicates that the "ratio (Long/Short)" is around 3, for the asymmetric dipoles(cf. for $\varrho \approx 10$km and L=5km for the long dipole), which is appreciably larger than the aforementioned value of 1.15 of the symmetric dipoles depicted in Fig. AI.13.

The above study was repeated for a two-layer earth having (the same basement with $\varrho_0 = 4 \times 10^3 \Omega$m but) with a thin (i.e., 50m) surface layer (ϱ_s=200Ωm or 10Ωm); the results are shown in Figs. AI.14 and AI.15 respectively. The general trend is that, upon adding a more conductive thin surface layer, the "ratio (Long/Short)" slightly decreases (for the same length of the long dipole and the same distance ϱ); for example, for AB≈8km, the "ratio (Long/Short)" decreases to ~1.2 (instead of 1.42 for the half-space in Fig. AI.13) when adding the surface layer of $\varrho_s \approx 10\Omega$m; note, however that, this value of ~1.2 is markedly smaller than the value of ~2 obtained (in Fig. AI.6a) for the same resistivity structure, but with asymmetric dipoles.

Case of $\varrho \approx 100$km: We again study the case of two symmetric dipoles (e.g., a short one A′B′=50m and a long one AB with variable length), but now located at a distance of $\varrho \approx 100$km from an emitting current dipole source (grounded on the earth's surface). Fig. AI.16 shows the results for a half-space with $\varrho_0 = 4 \times 10^3 \Omega$m, while Figs AI.17 and AI.18 correspond to a two-layer earth having the same basement resistivity (i.e., $4 \times 10^3 \Omega$m) but with surface layer's resistivities of 200Ωm and 10Ωm respectively. An inspection of Figs AI.16-18 shows that, for the usual length of ~5km of the long dipole, the "ratio (Long/Short)" is around unity.

For the sake of comparison, Figs AI.19-21 study the relevant case [for the same distance $\varrho \approx 100$km from the emitting source, i.e., a short dipole with (AB)=50m and a long one (AΓ) with variable length], but for the *asymmetric* dipoles (and the same dipole lengths). By considering the usual length of the long dipole, i.e. AΓ≈5km, we see that the "ratio (Long/Short)" is around 1.08 (see Figs AI.19a, AI.20a and AI.21a), if the emitting source and the remote electrode lie on the same side in respect to the measuring site (cf. when they lie on different sides -see Fig. AI.19b, AI.20b and AI.21b- the ratio is smaller than unity, as expected, i.e., around 0.93); in other words, in all these cases, the deviation from unity is around (3/2) x (AΓ)/ϱ only.

Before concluding this section, the following important point should be recalled, when considering the typical case of a two layered earth, with a (relatively) resistive basement and a (thin) surface (more) conductive layer: once the distance between the emitting (surface) dipole source and the measuring site is drastically larger than the thickness of the surface layer (cf. Appendix III.B), the electric field value is (solely or mainly, depending on the distance) governed by the resistivity of the basement (and *not* on the resistivity just beneath the measuring site). This is important in the following sense: when doing VAN measurements, artificial noise may come from distances of a few to several kilometers (when the strength of the source is appropriately large). Let us now consider (the extreme case of) $\varrho \approx 10$km and compare the right vertical scales of Figs AI.13 and AI.14; for a half-space ($\varrho_0=4\times10^3\Omega$m) the electric field value, produced by a noise source of ~1Am, is ~1.3nV/m; this value is slightly reduced to ~1.2nV/m, when considering a two layered earth (with the same basement $\varrho_0=4\times10^3\Omega$m, but) with a surface layer (~50m thickness) having conductivity 20 times larger than that of the basement (if $\varrho_s=10\Omega$m, the field is reduced ~0.3nV/m, i.e., it decreases by a factor of ~4-5 only -see Fig. AI.15- although the surface layer became 400 times more conductive than the basement).

As a general conclusion of this section we may say the following: when using a combination of short dipoles (L~50m) and long dipoles (L~5km), there is a *substantial* difference between the two cases: (i) *symmetric* and (ii) *asymmetric* dipoles (cf. especially when considering the configurations repeatedly recommended by VAN, e.g., when the emitting *surface* source and the remote electrode lie on the same side, in respect to the measuring site, or simply when the remote electrode is installed very close to the *surface* noise source); for noise source distances of ϱ~10km, the "ratio (Long/Short)" differs drastically from unity, e.g. it is ~3, for the asymmetric configuration (cf. the case of Fig. AI.4a), but only ~1.15 for the symmetric one; this emphasizes the *decisive role of the long dipoles* (cf. *asymmetric configuration*) in recognizing the noise emitted from nearby artificial sources. For large distances, e.g., $\varrho \approx 100$km (as in the case of SES, artificial noise cannot be detected at such distances), the "ratio (Long/Short)" slightly differs from unity and hence the ΔV/L-values either of the short dipoles or of the long ones represent the true electric field (which is mainly governed by the basement resistivity; note, however, that in the frame of the model of the SES transmission presented in this paper, the SES electric field

value also depends on the distance from the top of the channel, the conductance of the latter and, of course, on the measuring direction in respect to that of the channel, see below).

Study of the ΔV/L-values when two (almost parallel) long dipoles are operating simultaneously with a short dipole array.

We now turn to the case of two long dipoles ΑΓ′ and ΑΓ (e.g., with lengths 2km and 5km respectively) which are simultaneously operating with a short dipole AB, e.g., 50m (all these dipoles are assumed to be collinear). In order to study the possible sites (and orientations) of an emitting noise source (monopole or dipole) that produces signals having comparable ΔV/L-values (on the aforementioned 3 dipoles), we run a Monte-Carlo simulation. The position (and the orientation) of the monopole (or dipole) source is selected randomly within a circle of radius equal to (ΑΓ); the ΔV/L ratio is calculated (for each pair of dipoles) and if found to satisfy the condition (cf. for the three pairs of dipoles simultaneously):

$$|\Delta V/L \text{ ratio } -1| < \text{tolerance}$$

the program plots this solution on a graph, otherwise it continues with a new random selection of position (and orientation). The program ends when either 10000 solutions have been obtained or the CPU time limit (2 hours approximately in a CONVEX 3820 supercomputer) has been exceeded. In other words, in the aforementioned example, we searched for sites at which the following three inequalities were *simultaneously* satisfied:

$$|\text{ratio (Long/Short)}-1| < \text{tolerance, when } (\Lambda\Gamma)=5\text{km}, (\text{AB})=50\text{m}$$
$$|\text{ratio (Long}'\text{/Short)}-1| < \text{tolerance, when } (\Lambda\Gamma')=2\text{km}, (\text{AB})=50\text{m}$$
$$|\text{ratio (Long}'\text{/Long)}-1| < \text{tolerance, when } (\Lambda\Gamma')=2\text{km}, (\Lambda\Gamma)=5\text{km}$$

The results of the calculation (made either for a half-space, with $\varrho_o=4\text{x}10^3\Omega\text{m}$, or a two layered earth with $\varrho_o=4\text{x}10^3\Omega\text{m}$ and $\varrho_S=200\Omega\text{m}$) are depicted in Fig. AI.22, AI.23 and AI.24 by accepting a tolerance of 50%; the emitting noise source is assumed to be a monopole, a point (current) dipole and an extended (current) dipole (cf. with a length of 1km) respectively. An inspection of these figures indicates that a (dipole) noise source -after investigating its possible sites within a circle with a radius equal to the longer dipole- *cannot* lie at sites having the following coordinates:

(i) In front of the measuring site, i.e., x>0: a y-value between (ΑΓ)/2 and -(ΑΓ)/2 with a x-value between 0 and (ΑΓ) [cf. the same holds, but only approximately (due to the small shaded areas depicted in Fig. AI.22), for a monopole emitting source]; in other words, once we assured comparable ΔV/L-values on the two long dipoles (and on the short dipole as well), this indicates that *the noise source cannot lie within an area having dimensions almost* (ΑΓ)x(ΑΓ).

(ii) Backwards of the measuring site, i.e., x<0: within a semi circle with radius of, at least, (ΑΓ′)/2, or so.

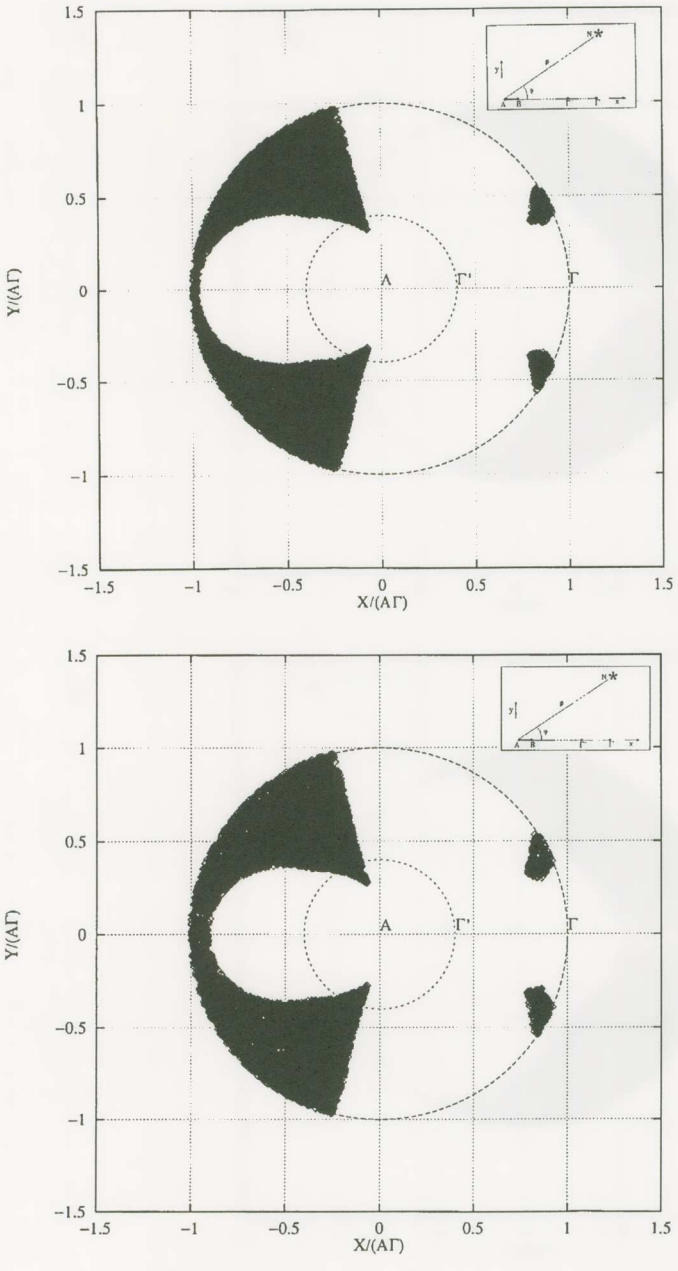

Fig. AI.22. Sites of a noise source (*monopole*) for which the ΔV/L values recorded by a short dipole and two long dipoles AΓ′ and AΓ are equal (with a tolerance 50%, see the text): a: half-space (ϱ_o=4x10^{3}Ωm); b: two layer earth (ϱ_S=200Ωm, ϱ_o=4x10^{3}Ωm).

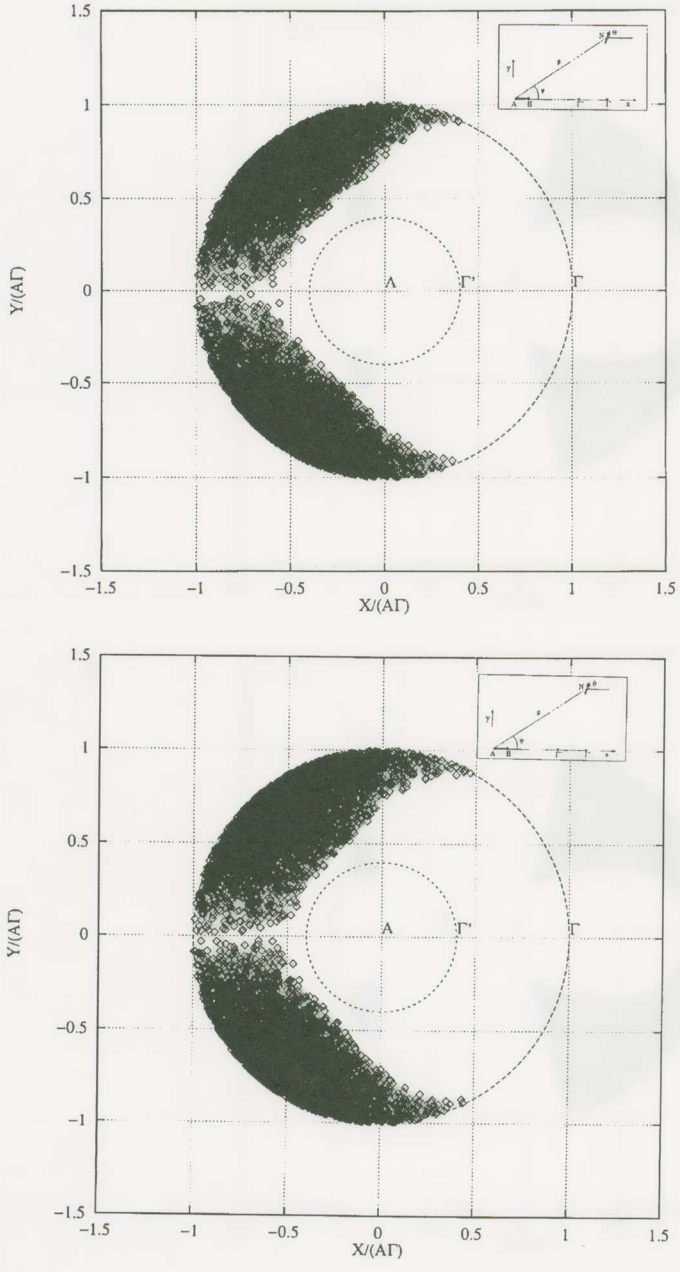

Fig. AI.23. Sites of a noise source (*point current dipole*) for which the ΔV-L values, recorded by a short dipole and two long dipoles AΓ′ and AΓ, are equal (with a tolerance 50%, see the text): a: half-space (ϱ_0=4x10^{3}Ωm); b: two layer earth (ϱ_S=200Ωm, ϱ_0=4x10^{3}Ωm).

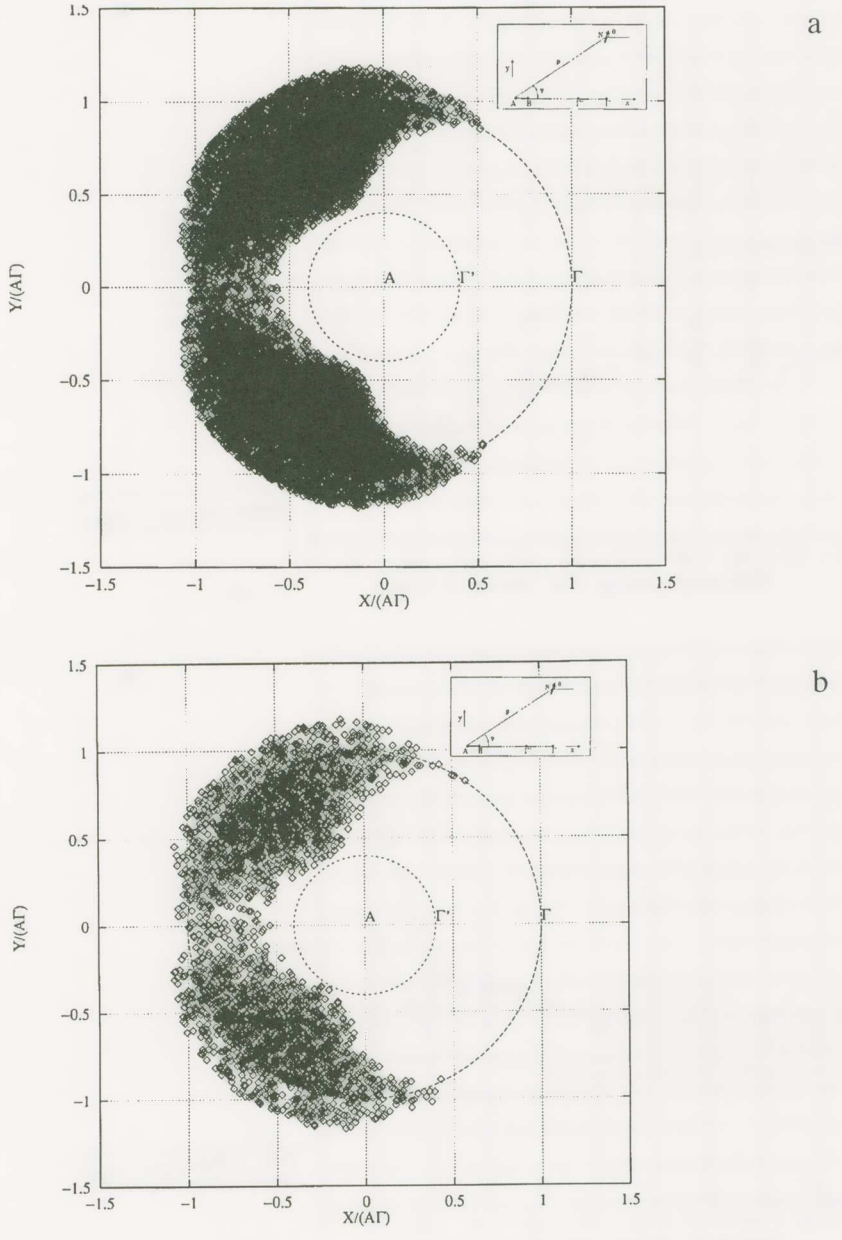

Fig. AI.24. Sites of a noise source (extended current dipole with a length of 1km) for which the ΔV/L values, recorded by a short dipole and two long dipoles AΓ′ and AΓ, are equal (with a tolerance 50%, see the text): a: half-space (ϱ_0=4x10^{3}Ωm); b: two layer earth (ϱ_S=200Ωm, ϱ_0=4x10^{3}Ωm).

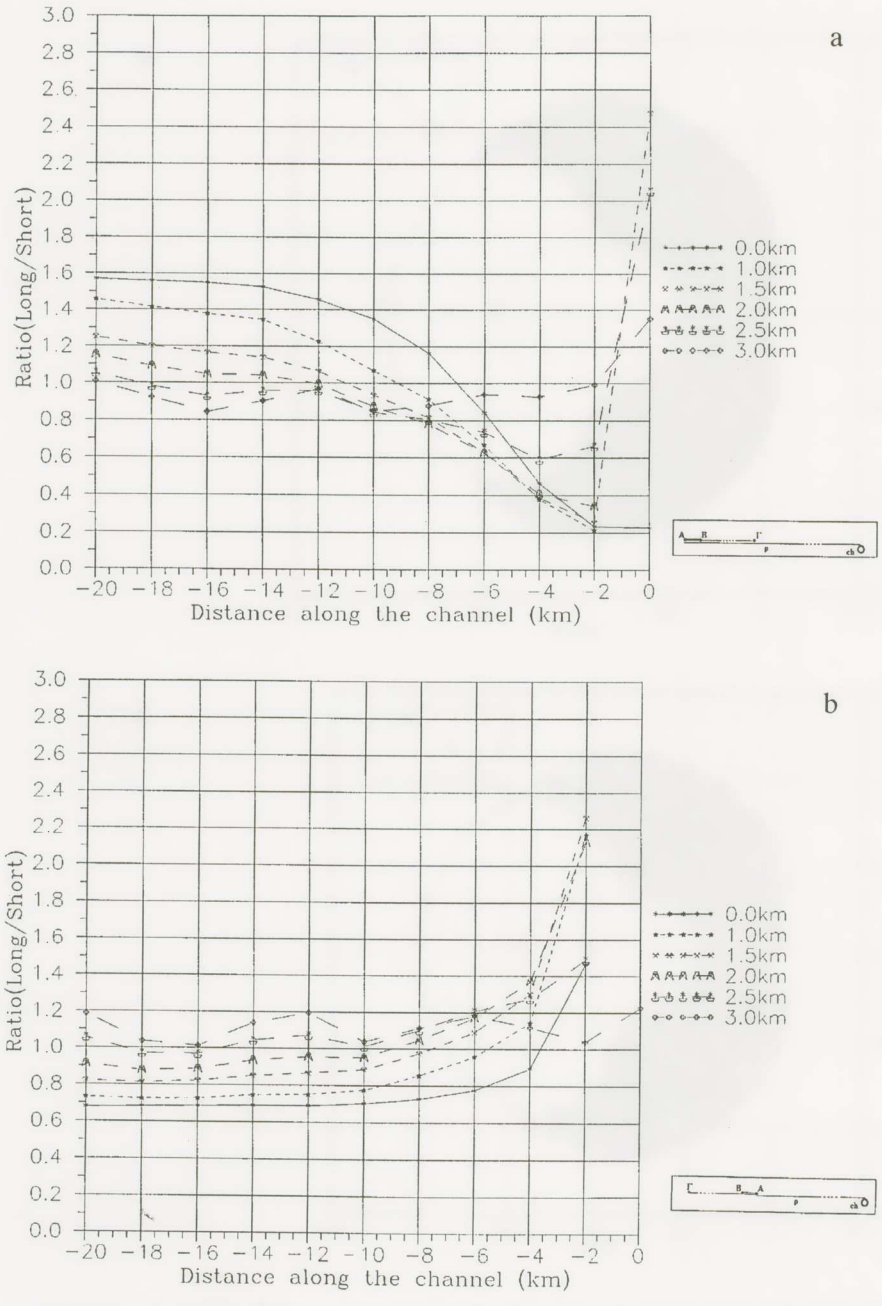

Fig. AI.25. Study of the "ratio (Long/Short)" for the SES transmission model discussed in the main text.

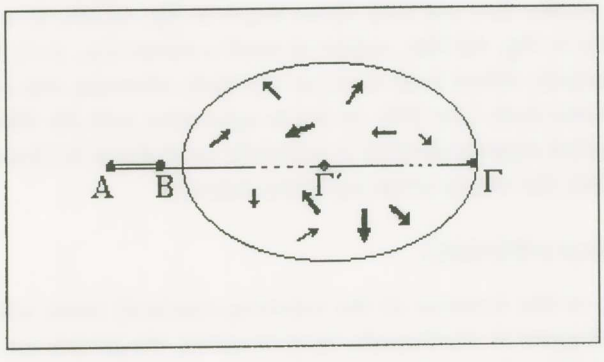

Fig. AI. 26. Configuration of a short dipole AB and two long dipoles AΓ΄ and AΓ for an easy recognition of noise; the emitting (noise) source is assumed to lie within the elliptical area.

Investigation of the validity of the ΔV/L-criterion in the case of the SES transmission model suggested in the main text.

Figs AI.25a,b show the "ratio (Long/Short)" for the *asymmetric* configuration of a long dipole (5km) and a short dipole (50m), at various distances (of the measuring site) from the projection on the earth's surface of the top of the channel; Fig. AI.25a corresponds to the case when the remote electrode and the top of the channel lie on the same side from the measuring site (i.e., the site of the short dipoles), while in Fig. AI.25b they lie on different sides. The (collinear) dipoles were assumed parallel to the projection of the channel on the earth's surface, at various y-values, i.e., y=0, 1.0, 1.5, 2.0, 2.5 and 3.0 km. An inspection of these figures shows the following: at short distances from the top of the channel (i.e., smaller than one long dipole length in Fig. AI.25b, or smaller than two long dipole lengths in Fig. AI.25a), and/or at small y-values (i.e., y≈0, 1.0), the "ratio (Long/Short)" markedly differs from unity, as expected; otherwise, this ratio *approaches unity* (it only deviates from 1 by 20%, or so) in agreement with the SES observations. (Note that a detailed experimentation is currently carried out in Greece in order to determine, if possible, the vicinity of the top of the channel).

Concluding remarks of APPENDIX I

Depending on the location of the emitting (surface) noise source (cf. in a homogeneous half-space or horizontally layered earth), the proper use of the ΔV/L-criterion can lead to the noise recognition as follows:

(1) In the case of a noise source N lying in the immediate vicinity of the short dipoles (*Varotsos and Lazaridou* [1991], see p.327), it can be easily recognised, because the cultural signal voltage ΔV does not generate the same field strength ΔV/L in neighbouring (short) dipoles with the same orientation but of different lengths. (This, of course, also excludes any electrochemical noise, arising from the instability of electrodes, e.g., due to rain).

(2) In the case of an artificial source the location of which is *known* and lies a few km (up to several km) away from the *measuring site*, the installation of a single long dipole (cf. in combination with a short dipole parallel to the long one) seems to be enough for the noise recognition, **if** its two electrodes are located as follows: one of them should be close to the measuring site, while the other, i.e., the remote one, should lie on the same side (cf. in respect to the measuring site) and the same straight line with the noise source; as for the exact location of this remote electrode, the following two possibilities are recommended:

(a) the noise source to lie closer to the measuring site than to the remote electrode [see Figs 12a,b by *Varotsos and Lazaridou*, 1991, or case II of Fig. 22 of *Varotsos et al.* 1993]; the noise is then easily recognised, because (irrespective of whether it comes from a monopole or dipole source) it gives signals with *opposite polarities* on the long dipole and on the (parallel) short dipole, i.e., the "*ratio (Long/Short)*" is negative,

(b) the noise source to lie close to the remote electrode (e.g., see Fig. 12c of *Varotsos and Lazaridou* 1991); the noise (irrespective of whether the emitting source is a monopole or a dipole) is then again easily recognised, because the "*ratio (Long/Short)*" differs drastically from unity (cf. in the case of an emitting dipole, the ratio is negative if it lies between the remote electrode and the measuring site; otherwise, it is positive, but it has a value significantly larger than unity).

(3) In the case of artificial sources (at distances up to several km from the measuring site), the exact location of which are *not known*, it is necessary to install *two* (almost parallel) long dipoles (cf. in addition to the short dipole array, one of the dipoles of which should be parallel to the long ones), with non equal lengths, but having one of their electrodes close to the measuring site; once the candidate area (for the tentative locations of artificial sources) can be roughly estimated, say an ellipse, care should be taken in order for its major axis to coincide, if possible, with one of the long dipoles, while the other dipole may have a smaller length, e.g., by a factor of 2, or so (see Fig. AI.26). Under such a configuration, any noise signal (emitted from the candidate area) *cannot give, as explained above, equal ΔV/L-values* (within a reasonable deviation of 50% or so) when comparing the long dipoles with their (parallel) short dipole(s).

APPENDIX II. SUMMARY OF THE ARGUMENTS THAT INVALIDATE GRUSZOW ET AL.'S [1996] CLAIMS.

On May 13, 1995, an earthquake (EQ) with magnitude 6.6 occurred in Kozani area (Greece). A prediction was issued well in advance by VAN, based on SES activities recorded at IOA (North-western Greece) on April 18 and 19, 1995. *Varotsos et al.* [1996b] published the corresponding SES and the relevant variations of the *horizontal* components of the magnetic field and commented on the latter that they are not significant. *Gruszow et al.* [1996] reported: (a) that they also observed (at a site labelled JAN E, 4.5km from the VAN station IOA, Fig. AII.1a) electrical variations simultaneously with those published by VAN, and (b) that the observed electrical variations were accompanied by magnetic field variations of ~1nT (measured at JAN M, lying 3.5 km from IOA, Fig. AII.1a). *Gruszow et al.* [1996] claim that their observations, as well as those of VAN, could be attributed to a (nearby) industrial source, with $Il = 1.6 \times 10^5 - 4 \times 10^4$ Am. It is the aim of this Appendix to prove that this *Gruszow et al.'s* [1996] claim contradicts *all* the observed results, including their own. In the main text we showed that it is naturally expected that very strong SES activities, like those preceded the 6.6 Kozani EQ, should be accompanied by magnetic field variations of 1nT, mainly on Z-component. Beyond this point, we shall indicate below the more definite errors of *Gruszow et al.* [1996]. (In the next two paragraphs, we follow their approximation that "the earth is represented by a half space with a conductivity $\sigma(z)$ depending only on the vertical coordinate").

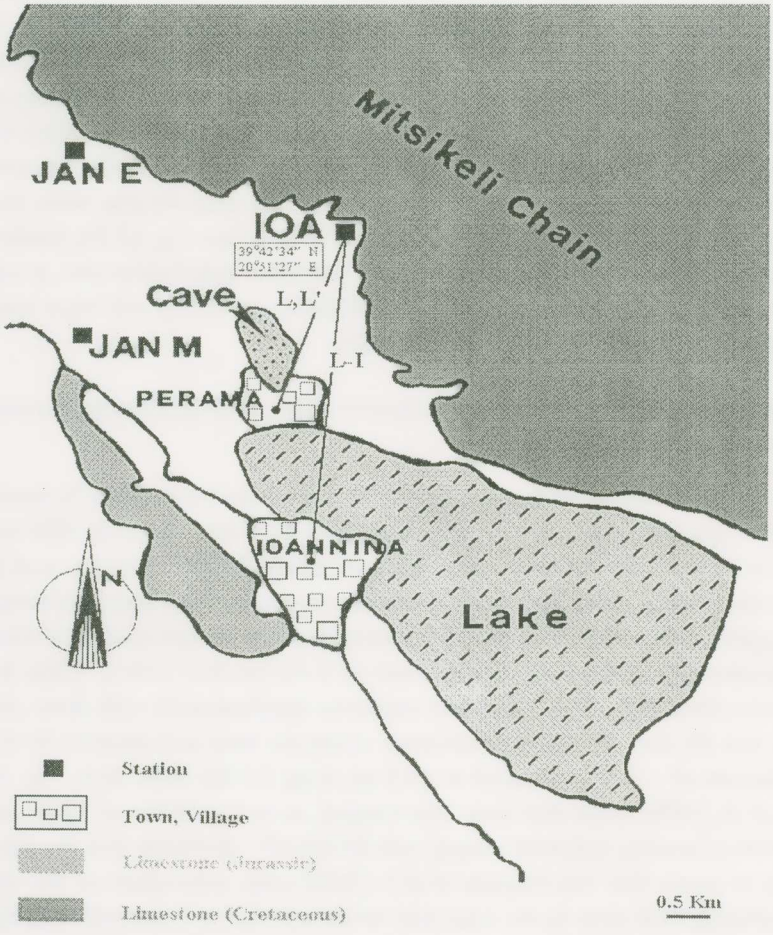

Fig. AII.1. Map showing the sites of JAN E and JAN M along with the long dipoles L, L′, and L-I at IOA (map a), and the short dipoles at IOA (map b).

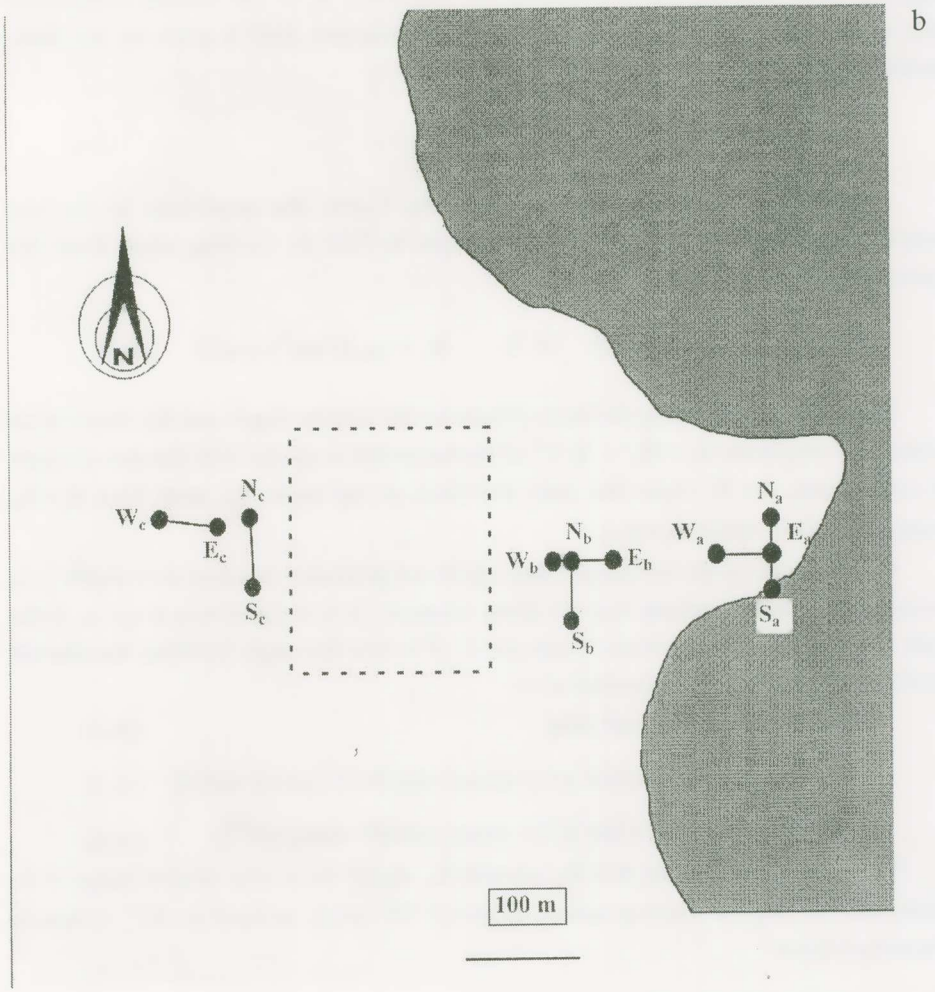
b
N
N_c
W_c
E_c
S_c
N_b
W_b
E_b
S_b
N_a
W_a
E_a
S_a
100 m

Non compatibility of the magnetic field observations of Gruszow et al. [1996] with nearby artificial sources

By recalling that *Gruszow et al.* [1996] observed that B_z is significantly larger than the horizontal component and following *Varotsos et al.* [1996d], we discuss below three possibilities for an eventual artificial source:

a) For a (surface) horizontal *point* current dipole (with current intensity I and length *l*), grounded at both ends (z=0), the amplitude B_z of the vertical component (due to the current flowing in the cable) of the magnetic field is given by the Biot-Savart law ($l<<r$):

$$B_z = (\mu_o Il/4\pi r^2) \sin\partial \qquad (A.1)$$

Assuming the current dipole is along the x-axis, the amplitude of the two components B_x and B_y of the horizontal magnetic field B_H (arising *solely* from the current flow in the earth) are:

$$B_x = (\mu_o Il/4\pi r^2) \sin 2\partial \quad (A.2) \qquad B_y = (\mu_o Il/4\pi r^2) \cos 2\partial \quad (A.3)$$

Therefore, when varying the angle ∂ between the current dipole and the observation vector **r** the amplitude $B_H=(B_x^2 + B_y^2)^{1/2}$ of the horizontal magnetic field remains constant (if r=constant), but B_z varies like $\sin\partial$; therefore, at any angle, we must have $B_z<B_H$ (except for $\partial=90°$, where $B_z=B_H$).

b) If the ends of the aforementioned dipole are grounded at a non zero depth $|z|$, Varotsos et al.[1996d] indicate that the above relations (A.1) to (A.3) turn to (cf. φ is the angle -smaller than 90°- between z-axis and **r** ; ∂ is now the angle between the current dipole and the horizontal component of **r**):

$$B_z = (\mu_o Il/4\pi r^2) \sin\partial \sin\varphi \qquad (A.4)$$

$$B_x = (\mu_o Il/4\pi r^2) [(1/\sin^2\varphi) (1-\cos\varphi) \sin 2\partial - (1/2)\cos\varphi \sin 2\partial] \qquad (A.5)$$

$$B_y = (\mu_o Il/4\pi r^2) [(1/\sin^2\varphi) (1-\cos\varphi) \cos 2\partial + \cos\varphi \sin^2\partial] \qquad (A.6)$$

These relations indicate that B_H exceeds B_z, except for a very narrow range of ∂-values (cf. for depths corresponding to $\varphi>23°23'$ only), around $\partial=90°$, which is determined from:

$$\sin^2\partial \sin^2\varphi (2\cos^2\varphi+4\cos\varphi+1) \geq 1 \qquad (A.7)$$

When this inequality holds, after considering that usually $|z| \sim$ m and r ~ km, we find that B_z/B_H exceeds unity [cf. within the angle $\partial=\pi/2\pm2(|z|/r)^{1/2}$ rad] by $\sim 2|z|/r$ only. For example, for $|z| \cong 2$m and $r \cong 4$km, B_z exceeds B_H (when $88° \lesssim \partial \lesssim 92°$, see Fig.

AII.2) by (at most) 1‰ ; such differences are below the experimental error, and hence observations cannot lead to B_z that (significantly) exceeds B_H.

c) For an *extended* current dipole (z=0), detailed calculations (Prof. R. Teisseyre, private communication) show that only in its vicinity (i.e., r<L) we may have that B_z significantly exceeds B_H (see Fig. AII.3); away from the dipole, B_z/B_H quickly drops to values smaller than unity (or ~1, if $\theta=90°$, while it approaches zero close to the dipole axis). Thus, when it is observed that B_z significantly exceeds B_H, this, in principle, could be attributed to an artificial source, only if situated quite near the measuring site; such a possibility, however, is excluded (see Appendix I) once the electric observations show that the (measuring) long dipoles (cf. almost with the same orientation and having one of their ends in the vicinity of the measuring short dipoles), resulted in approximately equal ΔV/L-values (compatible with the corresponding values of the short dipoles).

The above remarks indicate that the magnetic field observations of *Gruszow et al.* [1996] are not compatible with *any* of the aforementioned 3 possibilities of an artificial source. Furthermore, it is important to note that measurements we have conducted lately, at the *same* sites as *Gruszow et al.* [1996], demonstrated that disturbances from (nearby) industrial sources actually give $B_H>B_z$, thus precluding any possibility for their claim to be correct (e.g., even when considering nearby inhomogeneities); this experimental result, *alone*, invalidates *Gruszow et al'.s* [1996] claim about the magnetic signals being of cultural nature.

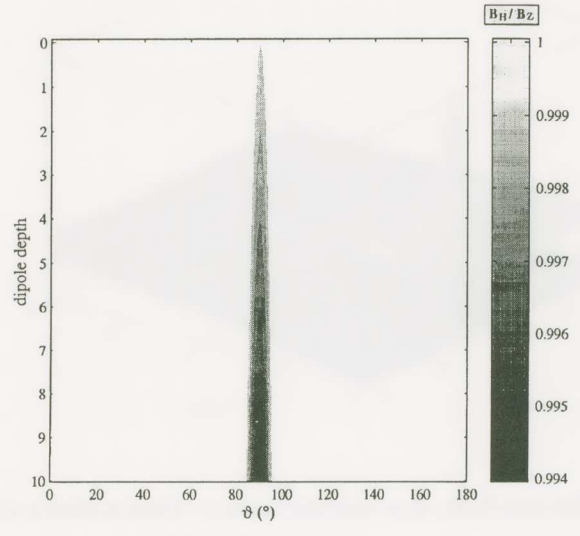

Fig. A. II.2. The shaded area shows, at various depths (for r=4km), the narrow angle, within which B_z slightly exceeds B_H (cf the corresponding value of the ratio B_H/B_z is shown to the right), for a buried current point dipole. Note that at z=0, at any angle, we must have $B_z<B_H$ (except for $\partial=90°$, where $B_z=B_H$).

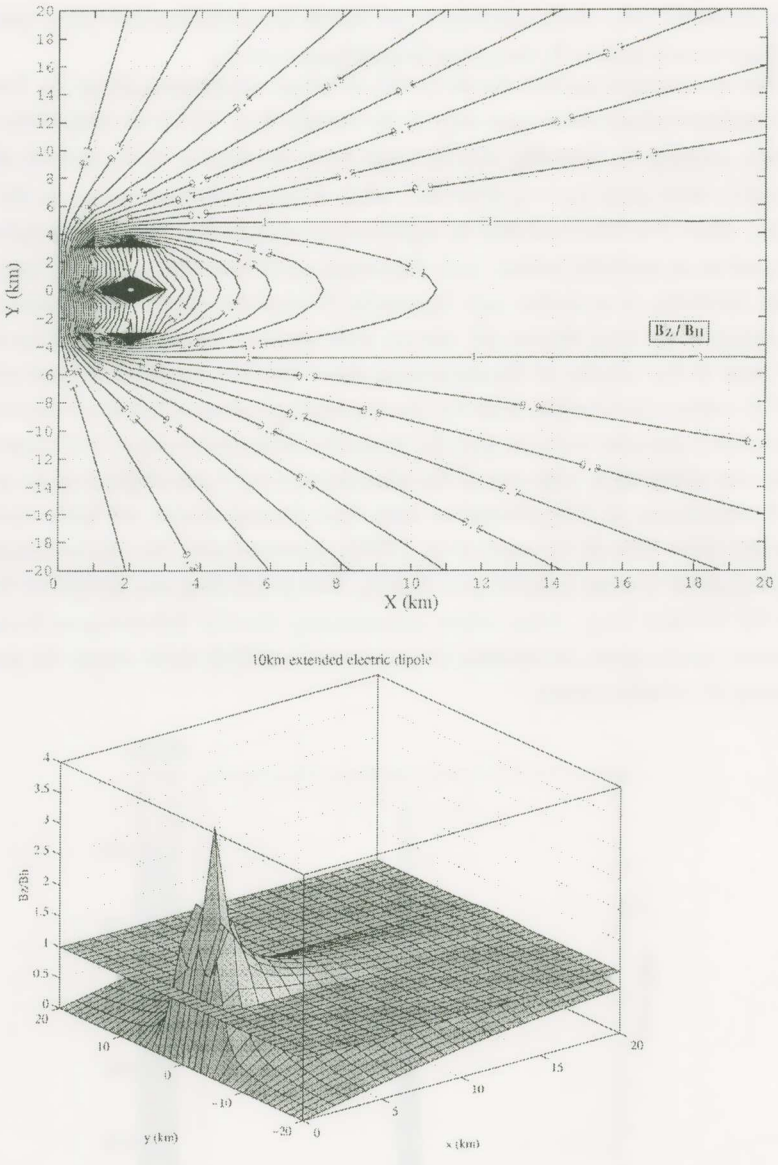

Fig. AII.3. The ratio B_z/B_H of an extended dipole (=10km) located at the origin of axis (and directed along y-axis).

Non compatibility of electrical observations with *Gruszow et al.'s* [1996] claim on nearby artificial sources

Gruszow et al. [1996] state that an industrial source with $Il=1.6\times10^5$Am is compatible with their B_z observation (at a distance R= 4km from JAN M). Concerning the distance r from JAN E and IOA to the source, they claim that "it seems safe to suppose that this distance is ...4 km". *Varotsos et al.* [1996c] presented the (horizontal) electric field variations, that would have been produced at JAN E and IOA by such an industrial source; the calculation was made by Berkeley's program (*Hoversten and Becker* [1995]) taking $Il\approx1.6\times10^5$Am, r≈4km, for a two-layered earth with a surface layer (thickness ~50 m) having resistivity $\varrho_s=200\Omega$m and a lower layer with $\varrho_0\approx4\times10^3\Omega$m (cf. These values are compatible, on the average, with the geoelectric structure around IOA [*K. Smith*, private communication] and with the detailed MT study by *Makris* [1996]). The results showed that electric field variations of the order of 1.5 to 2.6 V/km would have been measured at JAN E and IOA; these values are roughly two orders of magnitude larger than those measured. We emphasize that, if we change the aforementioned resistivity values with other (reasonable) values, the calculated electric field values are still far larger than those measured (the measurements are depicted in Figs AII.4 and AII.5, see also below); note that, even if we consider the extreme case of $\varrho_s=10\Omega$m (thickness ~50m), Fig. AII.6 indicates that the calculated electric field becomes ~0.3V/km, which is still drastically larger than that registered. Such a sharp discrepancy cannot be attributed to the complicated (near surface) geoelectrical structure of IOA (and hence to the incompleteness of the aforementioned simplified theoretical calculation), because the experimental results showed (see Figs AII.4, AII.5) that the $\Delta V/L$-values of the long dipoles were compatible -but not exactly equal, as expected- with those of the short ones. Thus, in any case, *Gruszow et al.'s* [1996] claim contradicts *all* the electrical observations (including their own).

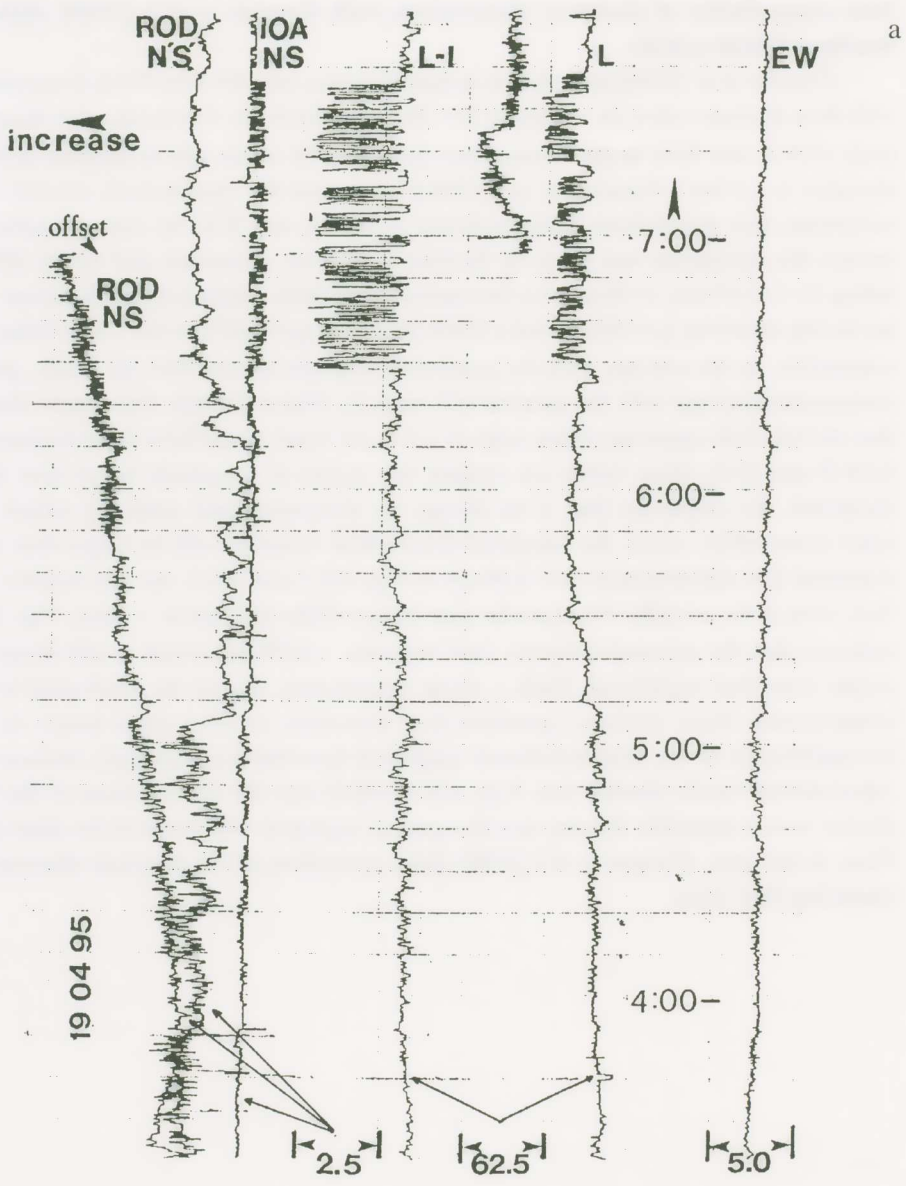

Fig. AII.4. SES activity at IOA on April 19, 1995. They are photocopies from the (continuous) analog recorders at the central station (GLY) of the real-time telemetric network (cf. the polarity of these recorders, as explained by *Varotsos et al.* [1993] with several examples, is opposite to that of a different type of recorders we use for additional dipoles operating at IOA). All channels correspond to IOA, except those labelled ROD or ASS which refer to other stations. The arrow, labelled increase, indicates the direction of increasing value of ΔV (e.g., see p. 324 of *Varotsos and Lazaridou* [1991]). All the scales are in mV.

b

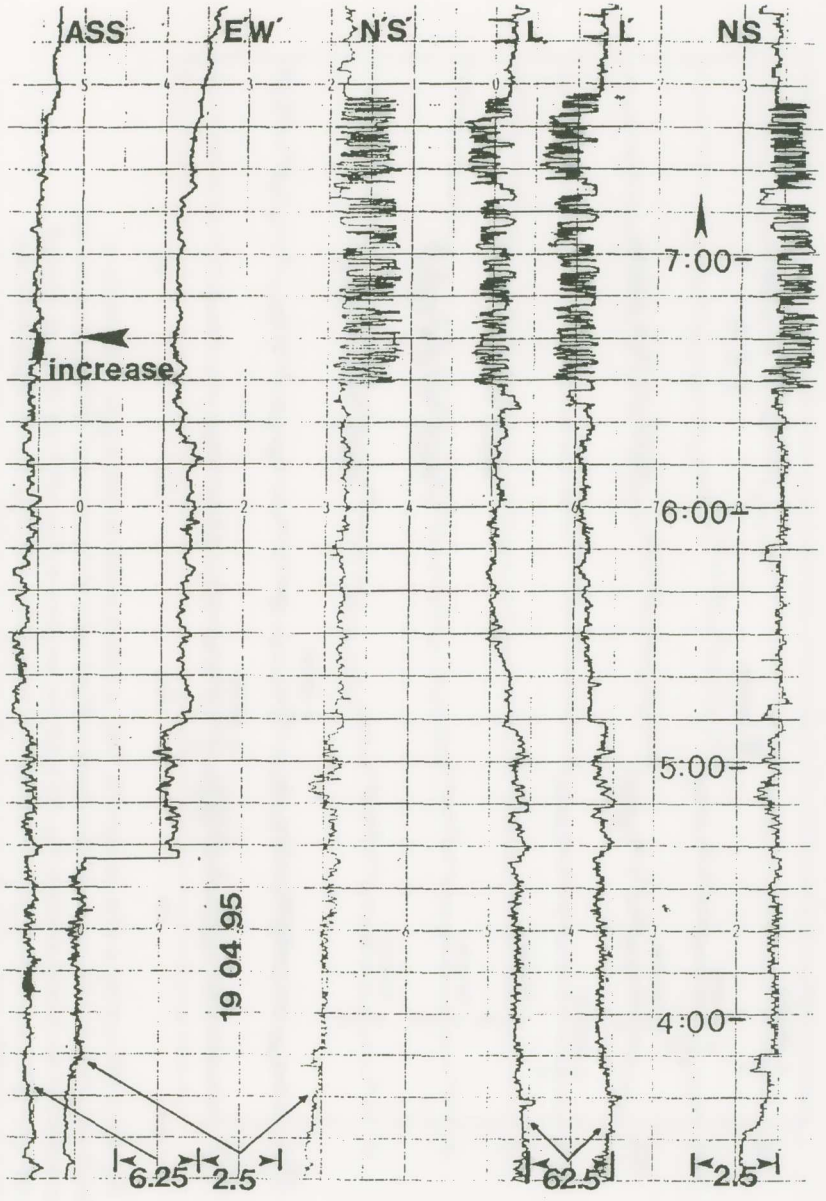

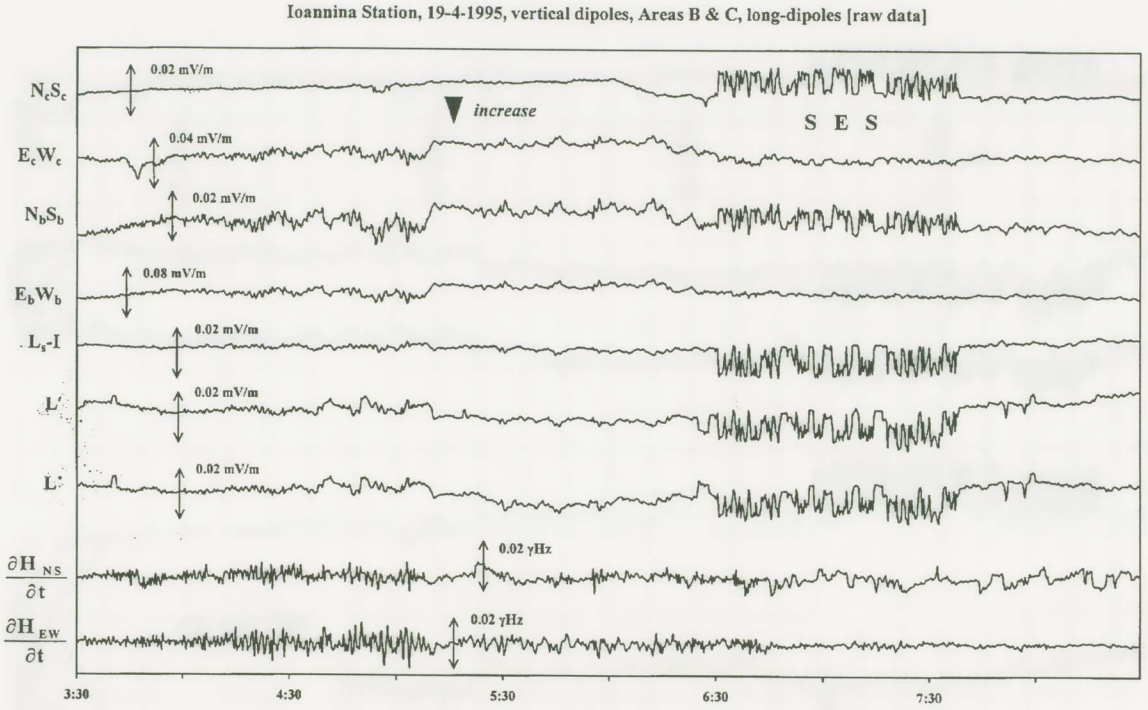

Fig. AII.5. SES activity at IOA on April 19, 1995, as collected with the data logger. The polarity at sites b and c (which is the same with that shown in Figs 5 and 6 of *Varotsos et al.* [1996b]) is *negative* in accordance to the records shown in Fig. AII.4. (cf. the recorders in Figs. AII.4 and AII.5 are span left and span right respectively); this is consistent with the polarity of the long dipoles which shows that the potential differences "IOA measuring site - Perama village", or "IOA measuring site - Ioannina city" *decrease*.

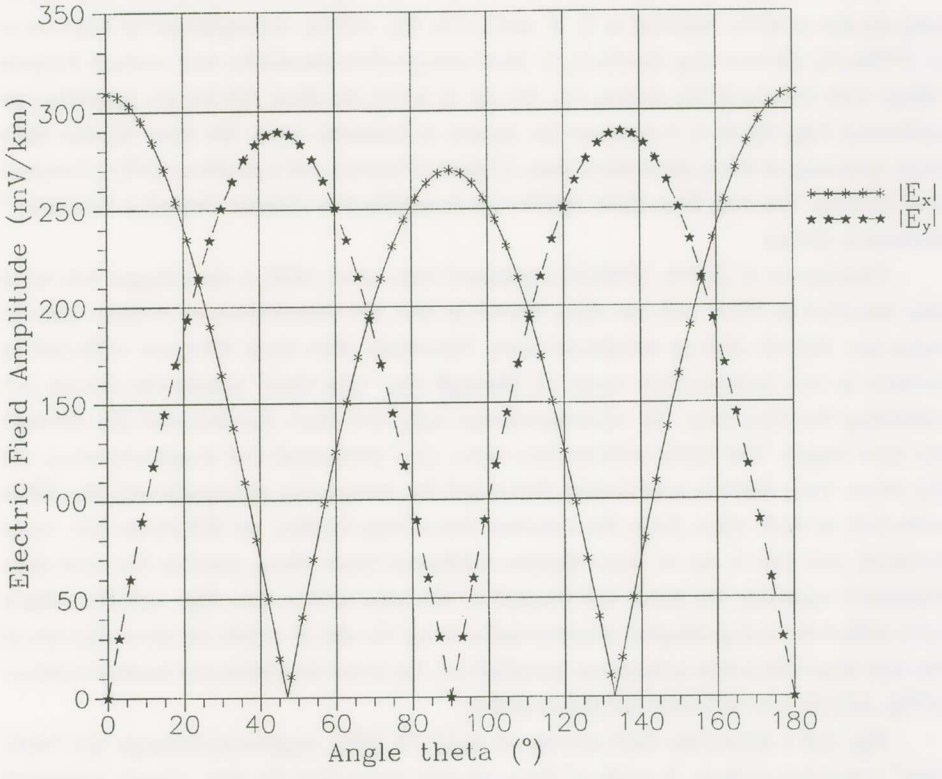

Fig. AII. 6. The amplitude of the two components of the electric field versus ∂ at a distance of 4km from a (point) current electric dipole with $Il = 1.6\times10^5$ Am grounded on the surface of a two layered earth ($\varrho_s=10\Omega$m with thickness 50m, $\varrho_0=4\times10^3\Omega$m).

Remarks on the validity of the four VAN criteria for the SES of Grevena-Kozani 6.6 EQ

In accordance with Fig. 21 of *Varotsos et al.* [1993], we have installed, long ago, 3 long dipoles at IOA, depicted as L, L΄ and L-I in Fig. AII.1a. As explained by *Varotsos et al.* [1996a,b], the two long dipoles L, L΄ have independent electrodes and connect Perama village with the site of the station, i.e., the site at which the short dipoles are operating; an additional long dipole L-I connects the station to Ioannina town. Six short dipoles have been operating at IOA, since more than 12 years (*Varotsos and Lazaridou* [1991]; *Varotsos et al.* [1993]). The data from these dipoles are transmitted to Athens through a "real time" telemetric system.

Varotsos et al. [1994, 1996a,b] explained that, since 1992, a data logger has been also installed at IOA, and the data, stored in situ, are transmitted to Athens once or twice per day via dial up telephone lines. Therefore, data from IOA are collected in Athens in two independent ways: (i) through the "real time" telemetric system (cf. collecting the data from the aforementioned long and short dipoles) and (ii) through the data logger. The latter collects data from: (i) 2 horizontal coil magnetometers, (ii) the three long dipoles mentioned above (cf. by comparing systematically the SESs collected, in both ways, from the *common* three long dipoles, no difference has been noticed) and (iii) a set of short dipoles (different from those used in the real time telemetric system); the latter are located at the sites a, b, c (see Fig. AII.1b), which have different local geological characteristics from the site at which the short dipoles of the real time telemetric system are installed (cf. the latter lie within the broken contour of Fig. AII.1b, i.e., between the sites b and c).

Fig. AII.4 shows the SES activity of April 19, 1995, registered through the "real-time" telemetric system. A study of these records shows that the four criteria published by *Varotsos and Lazaridou* [1991] are well obeyed. The following comments clarify a few points raised by *Gruszow et al.*[1996]:

(a) Concerning the "ΔV/L-criterion"; the three short dipoles (in the NS direction) with L=47.5 m, 100 m and 184 m (IOA, NS, in Fig. AII.4a, and NS and N΄S΄ in Fig. AII.4b) show almost the same ΔV/L-value (the dipoles, in EW direction, labelled EW and E΄W΄, have L=47.5 and 50m respectively). This invalidates *Gruszow et al.'s* [1996] claim that the criterion "ΔV/L = const" fails at IOA. Gruszow et al. [1996] incorrectly demand the equality of the ΔV/L -values of the NS-dipoles located at the different sites a, b and c, which have *different* directions of the electric field polarisation (*Varotsos et al.* [1994; 1996a,b]) deduced from MT measurements. We again emphasize that ΔV/L-test (for the short dipoles) should *not* be made in such cases of *inhomogeneous ground* (e.g., see pp. 324, 328 of *Varotsos and Lazaridou* [1991]).

(b) Concerning the SES polarity: for an easy recognition of the noise, coming from artificial sources inside (or close to) the long dipoles array, Varotsos and co-workers repeatedly emphasized that, for the configuration of the dipoles of the "real-time"

telemetric network, the following convention is used (e.g., see p. 343 of *Varotsos and Lazaridou* [1991]): "In measuring the potential difference between the electrodes of the short dipoles the following convention is used: E^+W^-, N^+S^-; and for the long dipole: (Perama village)$^+$ - (station)$^-$. This convention implies that for a true SES signal the *polarity* of ΔV for the long and parallel short dipole *should be opposite* [on the recording charts]". Therefore, Fig. AII.4 shows that the SES polarity on April 19, 1995 is negative. (The same holds for the SES of April 18, 1995). Recall that the prediction text (see Fig. 13a of *Varotsos et al.* [1996b]) emphasized that the SES characteristics (*polarity*, form, etc.) of the signals on April 18-19, 1995 are the same with those of Sept. 29, 1988 and Oct. 3, 1988 (cf. the polarity of the SES on October 3, 1988 was *negative*, e.g., see *Nagao et al.*[1996]). Furthermore, note that there is an obvious inconsistency in *Gruszow et al.* [1996], because in their Figs. 2a, 2b they plot correctly the (negative) SES polarity of the VAN signals, but in their Fig. 1b they plot this polarity in the opposite way.

Recapitulating, we have assured that all dipoles, short and long ones (directed almost in the NS direction), consistently show the *same (negative) polarity*. This fact excludes any possibility for attributing these signals to the "industrial areas: Perama village 2.5 km to the south-west of IOA, Ioannina town and suburbs 4 km to the south of IOA", because (e.g., see, Fig. 21 of *Varotsos et al.* [1993]) any disturbance, emitted from these industrial areas, should have destroyed (see Appendix I), either the internal consistency between the polarities of short and long dipoles, or it should have led to *drastically* different ΔV/L -values (see Fig. AII.5) of the long dipoles L, L′ and L-I, which was not the case.

The misuse of ΔV/L-criterion by *Gruszow et al.* [1996] at their electrical measurements

Gruszow et al [1996] mentioned that their ΔV/L -values (for the SESs of April 18-19, 1995) on their two NS dipoles are different and considered it in favour of an industrial origin of the disturbances; this is not so, because, either an industrial source lying at $r \approx 4$ km (i.e., at a distance far larger than the lengths of their short dipole array), or a natural EQ source at $r \approx 80$km, should give $\Delta V/L \approx$ constant, for their short dipoles, in a given direction, provided that their area is homogeneous (e.g., *Varotsos* and *Lazaridou* [1991]). Therefore, the inequality of ΔV/L -values should have instigated *Gruszow et al.* [1996] to study the inhomogeneity at their measuring site in a similar fashion as *Varotsos et al.* [1994, 1996a,b] did for the areas a, b and c at IOA (and found that their directions, along which the electric field is polarized, are different). In order to investigate the eventual inhomogeneity, *Varotsos et al.* [1996c] undertook a detailed MT survey, inside and just outside the array of *Gruszow et al* [1996]. Our results actually showed the existence of strong inhomogeneities. In other words, *Gruszow et al.* [1996] misused the criterion "ΔV/L =const", i.e., without checking if their measuring site is homogeneous.

Concluding remarks of Appendix II

The claim of *Gruszow et al.* [1996], i.e., the electrical signals on April 18-19, 1995 could be attributed to a nearby (huge) industrial source (cf. no such disturbances were reported by the Electrical Company), is in sharp contradiction to the theory as well as to *all* the experimental facts. First, their magnetic field measurements, detected a vertical variation, which is appreciably larger than the horizontal; this invalidates their claim, because, as we showed, a (nearby) industrial source cannot give (cf. at distances claimed by *Gruszow et al.* [1996]) a vertical magnetic field variation significantly greater than the horizontal one. Second, the strength of the (industrial) source, necessary to produce the detected B_z variation, would give an electric signal far stronger than the registered. Third, the totality of the electric field measurements, at short dipole arrays and at the long dipoles, preclude *any possibility* of an industrial origin of the electrical variations, because not only they *all* showed the same polarity, but also the long dipoles registered comparable $\Delta V/L$-values (which were also compatible with those of the short ones). Furthermore, note that *Gruszow et al.* [1996] misused the "$\Delta V/L$-criterion", because they required constant "$\Delta V/L$-values" (for short dipoles in a given direction), when comparing sites which (as we experimentally confirmed) exhibit different directions of electric field polarization.

APPENDIX III. SOLUTION OF THE BOUNDARY VALUE PROBLEMS: CONDUCTIVE CYLINDER OR CONDUCTIVE LAYER EMBEDDED IN A LESS CONDUCTIVE MEDIUM

A. CONDUCTIVE CYLINDER INSIDE A MEDIUM WITH SMALLER CONDUCTIVITY.

Point current source in the center of the cylinder

Let us suppose that the point current source is located at the origin (0,0,0) of a cylindrical system of coordinates. We also assume that a conductive cylinder (with conductivity σ) has its axis along the z-axis of the coordinate system and that it lies in the region $\rho<R$. The remainder of the space is a medium with smaller conductivity σ', i.e. $\sigma'<\sigma$. The electrostatic potential φ is composed of two parts: the primary part φ^p that is the (singular at the origin) potential of a point current source inside a full space of conductivity σ and a secondary part φ^s that is due to the existence of the cylinder. The primary potential can be written as

$$\varphi^p=I/[4\pi\sigma(\rho^2+z^2)^{1/2}]=I/(2\pi^2\sigma R)\int_0^\infty K_0(\xi\rho/R)\cos(\xi z/R)\,d\xi$$

since $\int_0^\infty K_0(\lambda\rho)\cos(\lambda z)\,d\lambda=\pi/[2(\rho^2+z^2)^{1/2}]$ (*e.g.*, see Abramowitz and Stegun, *Handbook of Mathematical Functions*, Dover, New York, [1970]).

Inside the cylinder the solution involves, the singular part φ^p ,that descibes the point current source, and the secondary part φ^s expressed in terms of the (well-behaving at the origin) modified Bessel function of the first kind $I_0(\xi\rho/R)$ (*J.R.Wait,Colorado School of Mines Quarterly* [1978], Vol.73, p. 1-21) :

$$\varphi_{IN}= \varphi^p +\varphi^s= I/(2\pi^2\sigma R) \int_0^\infty [K_0(\xi\rho/R)+A(\xi)I_0(\xi\rho/R)] \cos(\xi z/R)\, d\xi. \quad \text{III.1}$$

Outside the cylinder, the potential involves only the (well-behaving at infinity) modified Bessel function of the second kind $K_0(\xi\rho/R)$ *J.R.Wait* [1978]):

$$\varphi_{OUT}= I/(2\pi^2\sigma R) \int_0^\infty B(\xi)\, K_0(\xi\rho/R)\cos(\xi z/R)\, d\xi. \quad \text{III.2}$$

The unknown functions $A(\xi)$ and $B(\xi)$ are to be determined by the boundary conditions for the electric field $\mathbf{E}$=-grad φ on the surface of the cylinder ϱ=R:

$$E_{zIN}(z,R) = E_{zOUT}(z,R), \quad \text{III.3}$$

$$\sigma E_{\rho IN}(z,R) = \sigma' E_{\rho OUT}(z,R). \quad \text{III.4}$$

Equation III.3 implies

$$K_0(\xi)+A(\xi)\, I_0(\xi)=B(\xi)\, K_0(\xi), \quad \text{III.5}$$

and Eq.III.4, using, $K_0'(\xi)=- K_1(\xi)$ and $I_0'(\xi) = I_1(\xi)$, leads to:

$$\sigma\, K_1(\xi)-\sigma\, A(\xi)\, I_1(\xi)=\sigma' B\, (\xi)\, K_1(\xi). \quad \text{III.6}$$

A combination of, Eqs.III.5 and III.6 gives:

$$A(\xi)=(\sigma-\sigma')\, K_1(\xi)\, K_0(\xi)/[\sigma\, I_1(\xi)\, K_0(\xi)+\sigma'\, I_0(\xi)\, K_1(\xi)], \quad \text{III.7}$$

and

$$B(\xi)= 1+A(\xi)\, I_0(\xi)/\, K_0(\xi). \quad \text{III.8}$$

By inserting Eqs.III.7 and III.8 into Eqs.III.1 and III.2, respectively, we find the *electrostatic* potential inside and outside the cylinder.

The case of a dipole current source

We consider the case of a dipole current source $\mathbf{p}=I\mathbf{l}$, located at the origin. We first recall the general expression (*Zhdanov and Keller* [1994]) :

$$\varphi_{dipole}=-\mathbf{p}\ .\mathrm{grad}\ \varphi_{monopole}\ /I \qquad \text{III.9}$$

and then, using the expressions III.1 and III.2 (for the monopole potential), we can obtain the electrostatic potential for any polarization of the dipole.

For a dipole, $|\mathbf{p}|=Il$, along the z-axis, and for points inside the cylinder ($\varrho<R$) we obtain:

$$\varphi_{IN}(\rho,z)= Il/(2\pi^2\sigma R^2) \int_0^\infty [K_0(\xi\rho/R)+A(\xi)I_0(\xi\rho/R)]\ \xi \sin(\xi z/R)\ d\xi, \qquad \text{III.10}$$

while for points outside the cylinder ($\varrho>R$) we have:

$$\varphi_{OUT}(\rho,z)= Il/(2\pi^2\sigma R^2) \int_0^\infty K_0(\xi\rho/R)[1+A(\xi)I_0(\xi)/\ K_0(\xi)]\ \xi \sin(\xi z/R)\ d\xi. \qquad \text{III.11}$$

Fig.A.III.1 depicts, for various values of the distance d=z from the dipole, the ratio of the electric field E_z along the axis of the cylinder at $\varrho=0$ (labeled E_{inside}) over the electric field (along the same direction) for a full space of conductivity σ' at the same distance (labeled E_{host}). This ratio is plotted for various values of the conductivity contrast $\sigma/\ \sigma'$. Note that, for a given conductivity contrast, the ratio E_{inside}/E_{host} reaches a maximum value (larger than unity) at a certain reduced distance-denoted $(d/R)_{min}$ - and then decreases approaching unity at appreciably larger distances. If we recall that E_{host} varies with distance as $1/d^3$, we reach the following conclusion: when studying (reduced) distances *smaller than* $(d/R)_{min}$, the electric field E_{inside} (i.e., inside an one dimensional conductive channel) decreases (versus distance) more slowly than $1/d^3$; on the other hand, when restricting our study to (reduced) distances just *larger* than $(d/R)_{min}$, the field E_{inside} decreases (versus the distance) *faster* than $1/d^3$. Finally, at distances *appreciably* larger than $(d/R)_{min}$, the field E_{inside} varies as $1/d^3$ (approaching E_{host}).

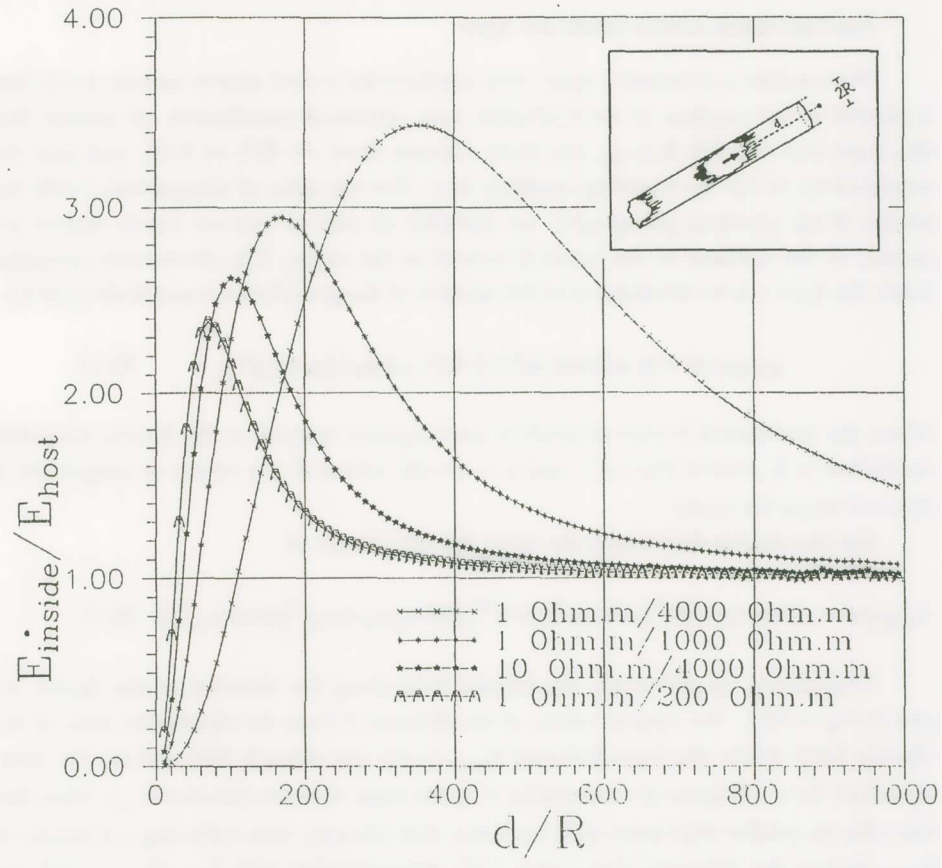

Fig. A.III.1. The ratio E_{inside}/E_{host} (*static*) versus the distance d from a current dipole lying inside a conductive cylinder (with radius R and conductivity σ) of infinite length embedded in a medium (host) with conductivity σ′(σ>σ′). The curves correspond to the following conductivity ratios: σ/σ′ = 4000/1, 1000/1, 4000/10 and 200/1 respectively.

B. CONDUCTIVE LAYER INSIDE A MEDIUM WITH SMALLER CONDUCTIVITY

Current dipole source inside the layer

We consider a conductive layer, with conductivity σ (and infinite surface area), that is parallel to the xy-plane of our Cartesian, now, system of coordinates; we assume that this layer has a width R (e.g., the layer extends from z=-R/2 to R/2), and that the conductivity of the surrounding medium is σ′. For the sake of comparison (with the results of the previous paragraph), we consider an electric current dipole source (cf. parallel to the surfaces of the layer) $\mathbf{I}l$ located at the origin. The electrostatic potential inside the layer can be determined by the method of images (*Zhdanov and Keller* [1994]):

$$\varphi_{2DIN}(\mathbf{x})=l\,[\mathbf{I}.\mathbf{x}/(4\pi\sigma|\,\mathbf{x}|^3)+\Sigma\, K^{|n|}{}_{12}\,\mathbf{I}.\mathbf{x}_n/(4\pi\sigma|\,\mathbf{x}_n|^3)], \qquad \text{III.12}$$

where the summation is over all positive and negative integers n; the Kelvin reflection coefficient is $K_{12}=(\sigma-\sigma')/(\sigma+\sigma')$, and $\mathbf{x}_n= \mathbf{x}+n\mathbf{R}$, where $\mathbf{R}$ is a vector of magnitude R directed along the z-axis.

For the electric field inside the layer, Eq.III.12 leads to:

$$E_{2DIN}(\mathbf{x})= l\,\{[3(\mathbf{I}.\mathbf{x})\mathbf{x}-\mathbf{I}|\,\mathbf{x}|^2]/(4\pi\sigma|\,\mathbf{x}|^5)+\Sigma\, K^{|n|}_{12}[3(\mathbf{I}.\mathbf{x}_n)\mathbf{x}_n-\mathbf{I}|\,\mathbf{x}_n|^2]/(4\pi\sigma|\,\mathbf{x}_n|^5)\} \quad \text{III.13}$$

Considering, as previously, the electric field along the direction of the dipole, we plot in Fig.A.III.2, for various values of the distance d from the dipole, the ratio of the electric field inside the layer (labeled E_{inside}) over the electric field (along the same direction) for a full space of conductivity σ′ at the same distance (labeled E_{host}). Note that this ratio (is smaller than unity and) increases with distance, thus reflecting a decrease of E_{inside} (versus the distance) *slower* than $1/d^3$; approximating with $E_{inside}/E_{host} \propto d/R$ (cf. which approximately holds only for a certain part of the curves depicted in Fig. A.III.2) we find that, roughly, $E_{inside} \propto 1/d^2$.

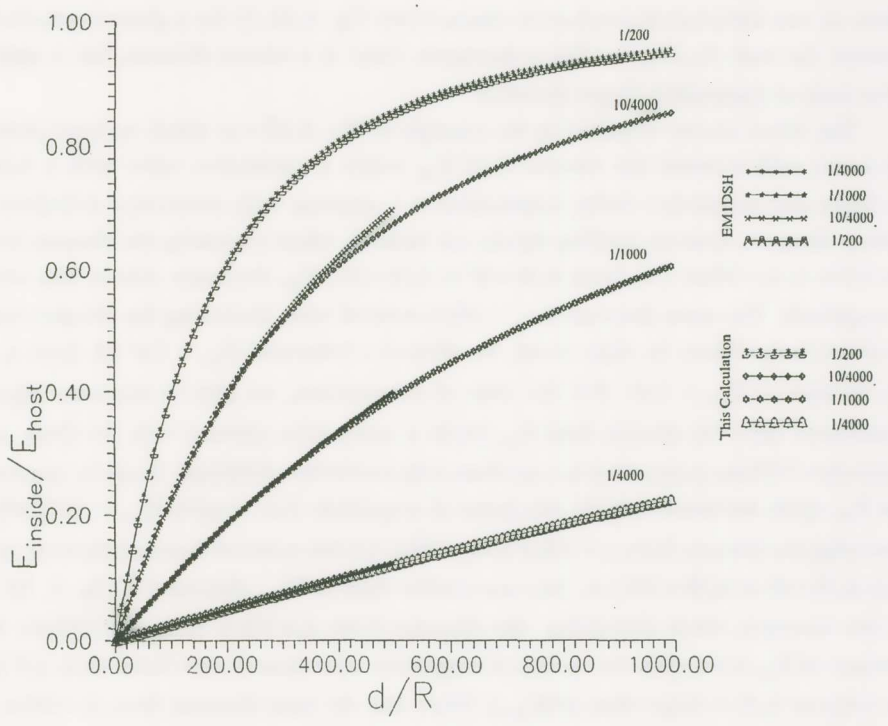

Fig. A.III.2. The ratio E_{inside}/E_{host} (*static*) versus the distance d from a current dipole lying inside a conductive layer (with width R, infinite surface area and conductivity σ), which is embedded in a medium (host) with conductivity σ′(σ>σ′). The curves correspond to the following conductivity ratios: σ′/σ= 1/4000, 1/1000, 10/4000 and 1/200 respectively. Each curve has been calculated in both ways, i.e., a) with the procedure described in the text (lower four symbols in the insert), and b) with EM1DSH program (upper four symbols in the insert); in the latter case we took advantage of the fact that the problem under discussion is equivalent with the following problem: a current dipole located at the surface of a two layer medium (consisting of a basement, with conductivity σ′, and a thin surface layer, with conductivity σ).

When comparing Figs (A.III.1) and (A.III.2) we conclude, as expected, that the electric field (E_{2D}) within a two-dimensional conductive layer is smaller than that (E_{1D}) within an one-dimensional conductive channel (see Fig. A.III.3); for a given conductivity contrast, the ratio E_{1D}/E_{2D} reaches a maximum value at a certain distance, but it approaches unity at appreciably larger distances.

The above can be visualised in the example of Fig. A.III.4 in which we have plotted (cf. curve with crosses) the electric field E_{2D} inside a conductive layer with a width R=500m and resistivity=10Ωm (embedded in a medium with resistivity=4000Ωm) at various distances from an emitting dipole; for instance, when increasing the distance from d_1=10km to d_2=30km (i.e., from d_1/R=20 to d_2/R=60), E_{2D} decreases only by one order of magnitude. The same decrease (i.e., ~10) is noticed when increasing the distance from d_2=30km to d_3=90km. In other words, we observe a behaviour $E_{2D} \propto 1/d^2$ (cf. from d_1 to d_3), instead of $E_{2D} \propto 1/d^3$. For the sake of comparison, we plot in the same figure (continuous line) the electric field E_{1D} inside a conductive cylinder with R=250m and resistivity=7.85Ωm (embedded in a medium with resistivity=4000Ωm). It can be observed that E_{1D} again decreases only by one order of magnitude (i.e., roughly $E_{1D} \propto 1/d^2$) when increasing the distance from d_1=10km to d_2=30km [cf. the reduced distances increase now from d_1/R=40 to d_1/R=120, i.e., they are smaller than $(d/R)_{min}$ discussed in Fig. A. III.1]; on the contrary, when increasing the distance from d_2=30km to d_3=90-100km, the decrease of E_{1D} is (roughly two orders of magnitude and hence) even faster than $1/d^3$ [cf. the value of d_3/R is larger than $(d/R)_{min}$]. (Note that the total decrease from d_1=10km to $d_3 \approx$90-100km is *smaller* than that expected from $1/d^3$). We draw attention to the following point: assume that in order to estimate the E_{1D} value, at d≈100km, one considers the (true) value at d≈ few km, and then applies the $1/d^3$ behaviour; such a calculation leads to an underestimation of E_{1D} (d ~ 100km) by (at least) one order of magnitude. This becomes obvious from the study of Fig. A.III.1 (when restricting to the cases between the two curves σ'/σ=1/1000 and σ'/σ=10/4000): for distances d/R≈10-20 the ratio E_{inside}/E_{host} is of the order of 10^{-1}, while at appreciably larger distances, i.e., d/R≈300-400, the ratio E_{inside}/E_{host} is larger than unity; in summary, when increasing the distance, e.g., from 4km to 100km, Fig. A.III 4 indicates that E_{1D} (or E_{2D}) decreases by 3 orders of magnitude *only* (note that the same decrease is found for E_{2D} if we consider, instead of an emitting point dipole, an *extended* dipole with length of 5km).

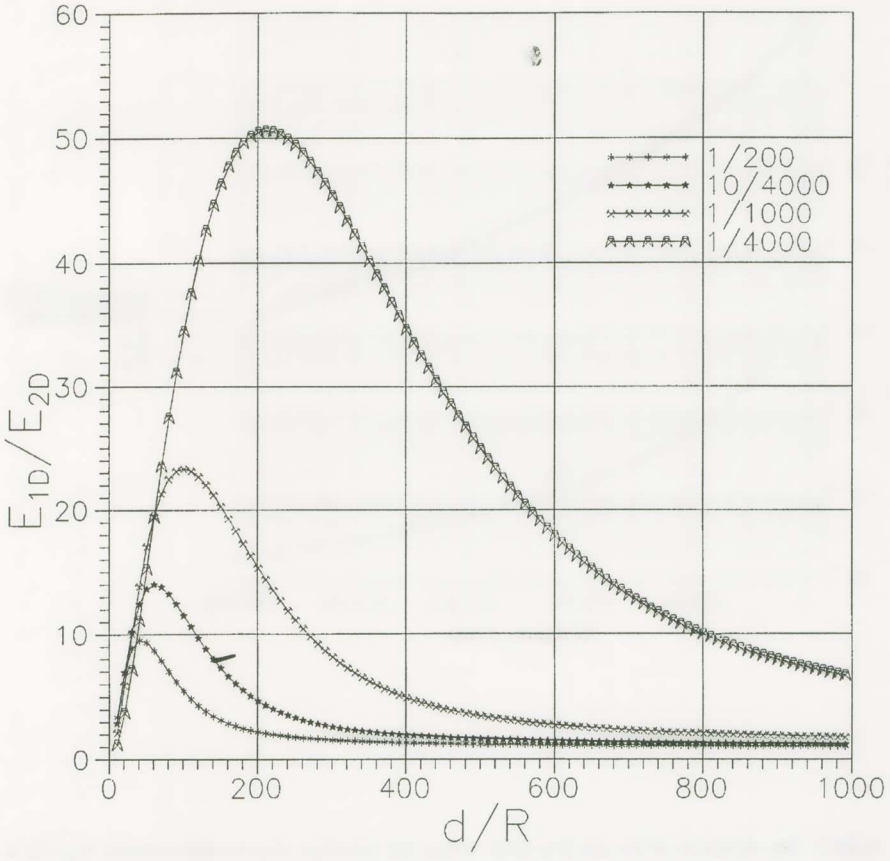

Fig. A.III.3. The ratio E_{1D}/E_{2D} (i.e. the electric field inside a conductive cylinder, with infinite length and radius R, over the electric field inside a conductive layer with width R and infinite surface) versus the distance d from a current dipole. The curves correspond to the following conductivity ratios: σ'/σ= 1/4000, 1/1000, 10/4000 and 1/200 respectively.

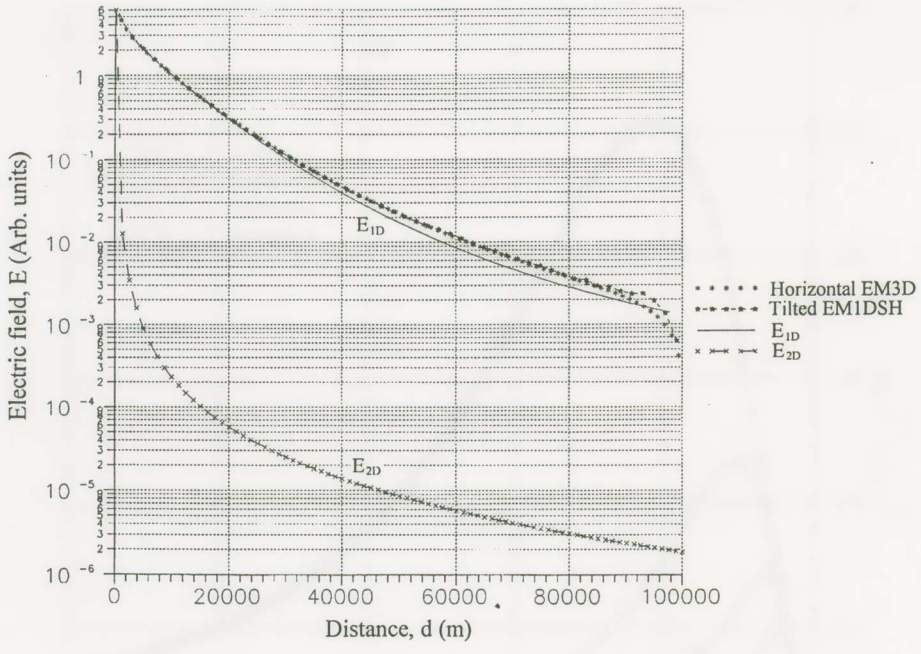

Fig. A.III.4. The decrease of the electric field versus the distance. Curve with crosses: E_{2D} for a conductive layer R=500m, resistivity=10Ωm (in a medium with resistivity=4000Ωm). Continuous line: E_{1D} for a conductive cylinder R=250m and resistivity=7.85Ωm [≈(π/2R)/50S] embedded in a medium with resistivity=4000Ωm; for the sake of comparison, we also depict the E_{1D} values calculated by: a) the EM1DSH program for the titled conductive channel (50 S) discussed in the text and b) the EM3D program (kindly forwarded by Prof. P. Wannamaker, Utah University) for a horizontal channel (50 S), with a length of 100km, lying at a depth of 5km in a two-layer earth (50m surface layer with ϱ_S=200Ωm on a basement with ϱ_0=4000Ωm)(cf. The E_{2D} and E_{1D} values should not be directly compared).

Acknowledgements. The first author would like to express his sincere thanks to Prof. K. Alexopoulos, Prof. Seiya Uyeda and Prof. David Lazarus for very useful discussions on the subject of the main text. We also thank Prof. Frank Morrison who drew our attention to the development of the EM1DSH program? we also acknowledge, with pleasure, the continuous help of Dr. M. Hoversten, in the application of this program. Useful discussions with Prof. F. Hadjioannou and A. Lahanas are greatly appreciated.

REFERENCES

Bernard, P., J.L. Le Mouel, On electrotelluric signals, in *The Critical Review of VAN: Earthquake Prediction from Seismic Electric Signals*, ed. Sir J. Lighthill, World Scientific Publishing Co., Singapore, 118-152, 1996.

Fraser-Smith, A.C., A. Bernardi, P.R. McGill, M.E. Ladd, R.A. Helliwell, and O.G. Villard, Jr., Low-frequency magnetic field measurements near the epicenter of the Ms 7.1 Loma Prieta earthquake, *Geophys. Res. Lett.*, 17, 1465-1468, 1990.

Gruszow, S., J.C. Rossignol, A. Tzanis, and J.L. Le Mouel, Identification and analysis of electromagnetic signals in Greece: the case of the Kozani earthquake VAN prediction, *Geophys. Res. Lett.*, 23, 2025-2029, 1996.

Hadjicontis, V., and C. Mavromatou, Laboratory investigation of the electric signals preceding earthquakes, in *The Critical Review of VAN: Earthquake Prediction from Seismic Electric Signals*, ed. Sir J. Lighthill, World Scientific Publishing Co., Singapore, 105-117, 1996.

Hoversten, G.M., and A. Becker, EM1DSH with EMMODEL a Motif GUI, *Numerical Modeling of multiple thin 3D sheets in a layered earth*, University of California at Berkeley, Engineering Geoscience Department, (June 12, 1995).

Lazarus, D., Note on a possible origin for seismic electric signals, *Tectonophysics 224*, 265-267, 1993.

Lazarus, D., Physical mechanisms for generation and propagation of seismic electrical signals, in *The Critical Review of VAN: Earthquake Prediction from Seismic Electric Signals*, ed. Sir J. Lighthill, World Scientific Publishing Co., Singapore, 91-96, 1996.

Makris, J., Magnetotelluric inspection of Ioannina area, PhD Thesis, University of Athens, 1996.

Morgan, D., A model for the explanation of SES-generation based on electrokinetic effect, paper presented at International Conference on Measurements and Theoretical Models of the Earths Field Variations Related to Earthquakes, Univ. Athens, Athens, Feb. 6 to Feb. 8, 1990.

Nagao, T., M. Uyeshima and S. Uyeda, An independent check of VANs criteria for signal recognition, *Geophys. Res. Lett., 23*, 1441-1444, 1996.

Park, S., M. Johnston, T. Madden, D. Morgan, and F. Morrison, Electromagnetic precursors to earthquakes in the VLF band: A review of observations and mechanisms, *Rev.Geophys.* 31, 117-132, 1993.

Park, S.K., D.J. Strauss, and R.L. Aceves, in *The Critical Review of VAN: Earthquake Prediction from Seismic Electric Signals*, ed. Sir J. Lighthill, World Scientific Publishing Co., Singapore, 267-285, 1996.

Slifkin, L., Seismic electric signals displacement of charged dislocations, *Tectonophysics 224*, 149-152, 1993.

Slifkin, L., A dislocation model for seismic electric signals, in *The Critical Review of VAN: Earthquake Prediction from Seismic Electric Signals*, ed. Sir J. Lighthill, World Scientific Publishing Co., Singapore, 97-104, 1996.

Teisseyre, R., Electric field generation in earthquake premonitory processes, *in Theory of Earthquake Premonitory and Fracture Processes*, edited by R. Teisseyre, pp. 282-303, Polish Scientific Publishers PWN Ltd, Warsawa, 1995.

Uyeda, S., Introduction to the VAN method of earthquake prediction, in *The Critical Review of VAN: Earthquake Prediction from Seismic Electric Signals*, ed. Sir J. Lighthill, World Scientific Publishing Co., Singapore, 3-28, 1996.

Varotsos, P., and K. Alexopoulos, Stimulated current emission in the earth and related geophysical aspects, in *Thermodynamics of Point Defects and their Relation with Bulk Properties*, edited by S. Amelinckx, R. Gevers and J. Nihoul, pp. 136-142, 403-406, 410-412, 417-420, North Holland, Amsterdam, 1986.

Varotsos, P., and M. Lazaridou, Latest aspects of earthquake prediction in Greece based on Seismic Electric Signals, *Tectonophysics 188*, 321-347, 1991.

Varotsos, P., K. Alexopoulos, and M. Lazaridou, Latest aspects of earthquake prediction in Greece based on seismic electric signals, II, *Tectonophysics 224*, 1-37, 1993.

Varotsos, P., K. Eftaxias, and M. Lazaridou, Recent VAN results (in Japanese), *Jishin Journal*, 17, 18-26, 1994.

Varotsos, P., K. Eftaxias, M. Lazaridou, G. Antonopoulos, J. Makris and J. Poliyiannakis, Summary of the five Principles suggested by Varotsos et al. [1996] and the additional questions raised in this debate, *Geophys. Res. Lett.*, 23, 1449-1452, 1996a.

Varotsos P., M. Lazaridou, K. Eftaxias, G. Antonopoulos, J. Makris and J. Kopanas, Short term earthquake prediction in Greece by Seismic Electric Signals, in *The Critical Review of VAN: Earthquake Prediction from Seismic Electric Signals*, ed. Sir J. Lighthill, World Scientific Publishing Co., Singapore, 29-76, 1996b.

Varotsos, P., N. Sarlis, N. Bogris, K. Eftaxias, M. Lazaridou, and P. Kapiris, Reply to Identification and analysis of electromagnetic signals in Greece: the case of the Kozani earthquake VAN prediction, by S. Gruszow et al., *Geophys. Res. Lett.*, 1996c (submitted for publication); see also pp. 503 of the Proceedings of AGU Fall Meeting 1996 (*EOS*, 77, No 46, Nov. 12, 1996).

Varotsos, P., K. Eftaxias, M. Lazaridou, K. Nomicos, N. Bogris, J. Makris, G. Antonopoulos and J. Kopanas. Recent earthquake prediction results in Greece based on the observation of Seismic Electric Signals. *Acta Geophysica Polonica*, Vol. XLIV, No. 4, 1996d

Zhdanov, M.S., and G.V. Keller. The Geoelectrical Methods in Geophysical Exploration. *Elsevier*, Amsterdam, 1994

Contents

Περίληψη

Ενα πιθανό πρότυπο για την εξήγηση της επιλεκτικότητας των Σεισμικών Ηλεκτρικών Σημάτων (SES)

Σε προηγούμενες δημοσιεύσεις, άλλες ερευνητικές ομάδες διατείνονται ότι για να ανιχνευθούν σεισμικά ηλεκτρικά σήματα (SES) σε επικεντρικές αποστάσεις r≈100km, πρέπει να εκπέμπονται ρεύματα τεράστιας έντασης, από την εστιακή περιοχή του επερχόμενου σεισμού. Σε αυτό το δημοσίευμα προτείνεται ένα πρότυπο, το οποίο εξηγεί ότι ακόμη και ρεύματα έντασης 1Α είναι ικανά να δώσουν ανιχνεύσιμα SES σε απόσταση r≈100km. Αυτό το πρότυπο αποδεικνύει ότι τα σήματα SES είναι ανιχνεύσιμα μόνο σε ορισμένες περιοχές,, εξηγώντας έτσι το φαινόμενο της *επιλεκτικότητας*. Επίσης αποδεικνύεται ότι μόνο για μεγάλους σεισμούς με μέγεθος 6.5-7.0 μπορεί να ανιχνευθεί μεταβολή του μαγνητικού πεδίου συνοδεύουσα τα SES. Αυτό ακριβώς παρετηρήθη στον σεισμό 6.6 της περιοχής Κοζάνης-Γρεβενών.

Επίσης, σε ένα ξεχωριστό Κεφάλαιο, δίδεται περιληπτικά η φυσική βάση του κριτηρίου ΔV/L=σταθερό. Αποδεικνύουμε ότι, όταν τα ηλεκτρόδια των διπόλων μεγάλου μήκους εγκαθίστανται κατάλληλα (δηλ. με έναν τρόπο που έχει προταθεί από το ΒΑΝ αρκετά χρόνια πριν), οι αντίστοιχες τιμές ΔV/L που οφείλονται σε τεχνητές πηγές εγκατεστημένες σε αποστάσεις έως και αρκετά χιλιόμετρα από το σημείο μέτρησης, διαφέρουν σημαντικά από τις αντίστοιχες τιμές των μικρών διπόλων και ως εκ τούτου οδηγούν σε μία εύκολη αναγνώριση του θορύβου.

Σε ένα επιπρόσθετο ξεχωριστό Κεφάλαιο συζητούμε τους ισχυρισμούς των Gruszow et al. [1996], δηλ. ότι τα SES που συσχετίζονται με τον σεισμό 6.6 Κοζάνης-Γρεβενών μπορούν να αποδοθούν σε μία κοντινή βιομηχανική πηγή η οποία εξέπεμψε ένα τεράστιο ρεύμα. Αποδεικνύουμε ότι ο ισχυρισμός αυτός είναι σε δυσαρμονία **και** με την θεωρία **και** με τα πειραματικά αποτελέσματα. Για παράδειγμα, εάν αυτά τα σήματα οφείλοντο σε βιομηχανική πηγή: (α) αυτά έπρεπε να συνοδεύονται με μαγνητικές μεταβολές κυρίως της οριζοντίου συνιστώσης, ενώ η παρατηρηθείσα μαγνητική μεταβολή κατεγράφη κυρίως στην κατακόρυφη συνιστώσα και (β) οι μεταβολές του ηλεκτρικού πεδίου θα έπρεπε να έχουν πλάτος δύο τάξεις μεγέθους μεγαλύτερο από αυτό που παρετηρήθη. Επί πλέον οι *Gruszow et al.* [1996] δεν εχρησιμοποίησαν ορθώς τα δεδομένα ΒΑΝ, π.χ. δεν εφήρμοσαν ορθώς το κριτήριο ΔV/L=σταθερό, και ως εκ τούτου **κανένα** από τα επιχειρήματά τους δεν ευσταθεί.